molecules

MDPI

Article

Design, Synthesis, In Vitro Biological Evaluation and In Silico Molecular Docking Study of Benzimidazole-Based Oxazole Analogues: A Promising Acetylcholinesterase and Butyrylcholinesterase Inhibitors

Rafaqat Hussain [1], Fazal Rahim [1,*], Hayat Ullah [2,*], Shoaib Khan [3], Maliha Sarfraz [4], Rashid Iqbal [5,6], Faiza Suleman [7] and Mohammad Khalid Al-Sadoon [8]

[1] Department of Chemistry, Hazara University, Mansehra 21120, Pakistan; rafaqathussain0347@gmail.com
[2] Department of Chemistry, University of Okara, Okara 56130, Pakistan
[3] Department of Chemistry, Abbottabad University of Science and Technology (AUST), Abbottabad 22500, Pakistan; shoaibkhanswati@gmail.com
[4] Department of Zoology, Wildlife and Fisheries, University of Agriculture Faisalabad, Sub Campus Toba Tek Singh, Faisalabad 36050, Pakistan; maliha.sarfraz@yahoo.com
[5] Department of Agroecology-Climate and Water, Aarhus University, Blichers Allé 20, 8830 Tjele, Denmark; rashid.iqbal@iub.edu.pk
[6] Department of Agronomy, Faculty of Agriculture and Environment, The Islamia University of Bahawalpur, Bahawalpur 63100, Pakistan
[7] Department of Botany, Government College University, Lahore 54000, Pakistan
[8] Department of Zoology, College of Science, King Saud University, P.O. Box 2455, Riyadh 11451, Saudi Arabia; msadoon@ksu.edu.sa
* Correspondence: fazalstar@gmail.com (F.R.); ayaanwazir366@gmail.com (H.U.)

Abstract: Alzheimer's disease (AD) is a degenerative neurological condition that severely affects the elderly and is clinically recognised by a decrease in cognition and memory. The treatment of this disease has drawn considerable attention and sparked increased interest among the researchers in this field as a result of a number of factors, including an increase in the population of patients over time, a significant decline in patient quality of life, and the high cost of treatment and care. The current work was carried out for the synthesis of benzimidazole-oxazole hybrid derivatives as efficient Alzheimer's inhibitors and as a springboard for investigating novel anti-chemical Alzheimer's prototypes. The inhibition profiles of each synthesised analogue against acetylcholinesterase (AChE) and butyrylcholinesterase (BuChE) enzymes were assessed. All the synthesized benzimidazole-based oxazole analogues displayed a diverse spectrum of inhibitory potentials against targeted AChE and BuChE enzymes when compared to the reference drug donepezil (IC_{50} = 2.16 ± 0.12 M and 4.50 ± 0.11 μM, respectively). The most active AChE and BuChE analogues were discovered to be analogues 9 and 14, with IC_{50} values of 0.10 ± 0.050 and 0.20 ± 0.050 μM (against AChE) and 0.20 ± 0.050 and 0.30 ± 0.050 μM (against BuChE), respectively. The nature, number, position, and electron-donating and -withdrawing effects on the phenyl ring were taken into consideration when analysing the structure-activity relationship (SAR). Molecular docking studies were also carried out on the active analogues to find out how amino acids bind to the active sites of the AChE and BuChE enzymes that were being studied.

Keywords: synthesis; benzimidazole; oxazole; AChE and BuChE; molecular docking study; structure-activity relationship

check for updates

Citation: Hussain, R.; Rahim, F.; Ullah, H.; Khan, S.; Sarfraz, M.; Iqbal, R.; Suleman, F.; Al-Sadoon, M.K. Design, Synthesis, In Vitro Biological Evaluation and In Silico Molecular Docking Study of Benzimidazole-Based Oxazole Analogues: A Promising Acetylcholinesterase and Butyrylcholinesterase Inhibitors. *Molecules* **2023**, *28*, 7015. https://doi.org/10.3390/molecules28207015

Received: 10 August 2023
Revised: 21 September 2023
Accepted: 22 September 2023
Published: 10 October 2023

Copyright: © 2023 by the authors. Licensee MDPI, Basel, Switzerland. This article is an open access article distributed under the terms and conditions of the Creative Commons Attribution (CC BY) license (https://creativecommons.org/licenses/by/4.0/).

1. Introduction

Alzheimer's disease is mainly caused by cholinesterase (AChE and BuChE) enzymes. These enzymes primarily work to hydrolyze acetylcholine into choline acetic acid [1]. These result in a lack of acetylcholine in the hippocampus and cortex of the brain, which are linked

to important psychological activities [2] and result in the development of Alzheimer's disease (AD), a persistent and irreversible brain illness. The cholinergic system of the brain continues to be affected, which frequently results in confusion, memory loss, cognitive impairment, difficulty solving problems, and thinking difficulties [3–5]. Additionally, because these enzymes are in charge of the neurotoxic β-amyloid accumulation that results in neuronal cell apoptosis, AD is the main cause of dementia in an ageing society. The best course of action for treating AD is to target both of these enzymes [6,7] by concentrating on the acetylcholinesterase enzyme, which has two binding sites: a peripheral location for the interaction of β-amyloid and a catalytic site for the hydrolysis of acetylcholine. In the form of the AChE-Aβ complex, it induces neurotoxicity as a result of its interaction with proteins. Furthermore, BuChE is mostly found in the heart, lungs, kidneys, liver, gut, and serum, whereas AChE is found in the cholinergic brain, neurons, and muscle [8,9]. The primary role of these enzymes is to break down substances that contain esters; AChE is predominant in the brain, and as acetylcholine activity gradually declines, BuChE function increases. To block the potential of these enzymes, a powerful medication is still required [10]. The FDA has approved a number of medications, including donepezil, rivastigmine, tacrine, and galantamine, for the treatment of Alzheimer's. Tacrine and Rivastigmine have been used to inhibit both AChE and BuChE, while Donepezil and Galantamine have been used to inhibit AChE [11] (Figure 1).

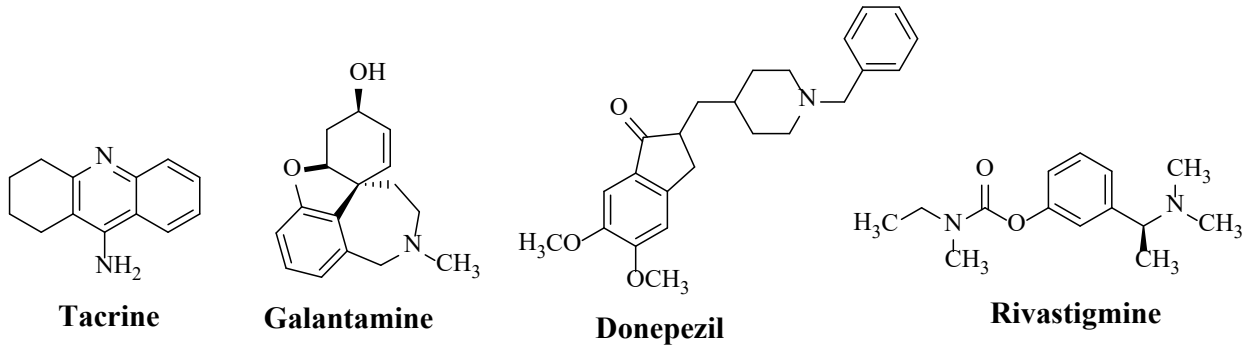


Figure 1. Available drug of AD with AChE inhibitory activity.

Antioxidants [12], anticancer agents [13], CNS stimulants [14], antiviral agents [15], anticoagulants [16], anti-inflammatory agents [17], anti-parasitic agents [18], anti-microbial agents [19], and blood pressure lowering agents [20] have all been found in benzimidazole and its derivatives. There are numerous bioactive drugs used in the market that contain benzimidazole skeletons in their structures, such as bandamustine, enviradine, astemizole, albendazole, and omeprazole (Figure 2) [21].

Oxazole scaffolds play a vital role in the design and development of several biologically active pharmaceutical drugs with interesting biological profiles, natural products, functional materials, and ligand frameworks [22]. Oxaprozin, aleglitazar, and aristoxazole (Figure 3) are examples of naturally occurring compounds that contain oxazole, which is a physiologically active scaffold [23,24].

We had already synthesized several N-containing heterocyclic compounds as potent inhibitors of alpha-amylase, alpha-glucosidase, urease, β-glucuronidase, thymidine phosphorylase, AChE and BuChE enzymes [25–27]. Furthermore, the molecular hybridization approach has been widely employed for the design and synthesis of hybrid analogues for the treatment of Alzheimer's disease. This approach mainly involves the combining of two or more than two different pharmacophore moieties in a single molecule having a common skeleton. These hybrid molecules may have advantages over standard drugs. In the current work, we used molecular hybridization to combine the biologically important two heterocyclic moieties; benzimidazole and oxazole, to obtain new hybrid molecules (Figure 4). As earlier discussed, both benzimidazole and oxazole moieties are very important for the treatment of Alzheimer's disease, and thus hybrid analogues containing benzimidazole

and oxazole moieties were synthesized and evaluated for their in vitro AChE and BuChE and molecular docking studies thereafter. Keeping in mind the biological importance of benzimidazole [28–30] and oxazole [31] scaffolds (Figure 4), in this study, we designed and synthesized hybrid analogues based on benzimidazole-bearing oxazole derivatives to further explore the AChE and BuChE inhibition profiles for the better treatment of Alzheimer's disease.

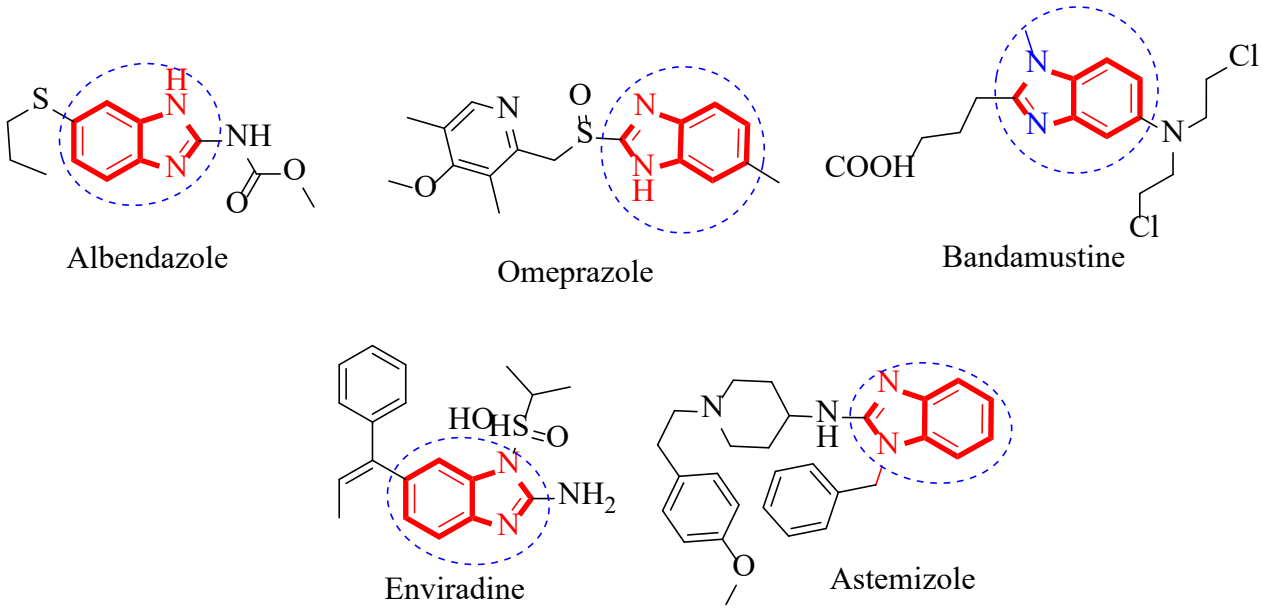


Figure 2. Drug comprising benzimidazole moiety.

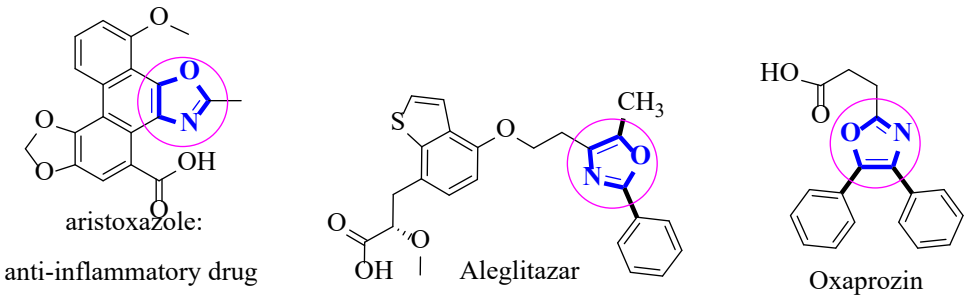


Figure 3. Bioactive drugs containing oxazole skeleton.

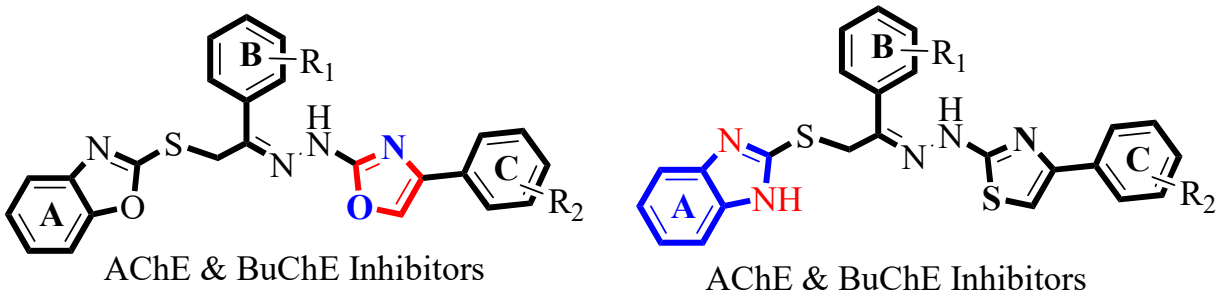


Figure 4. *Cont.*

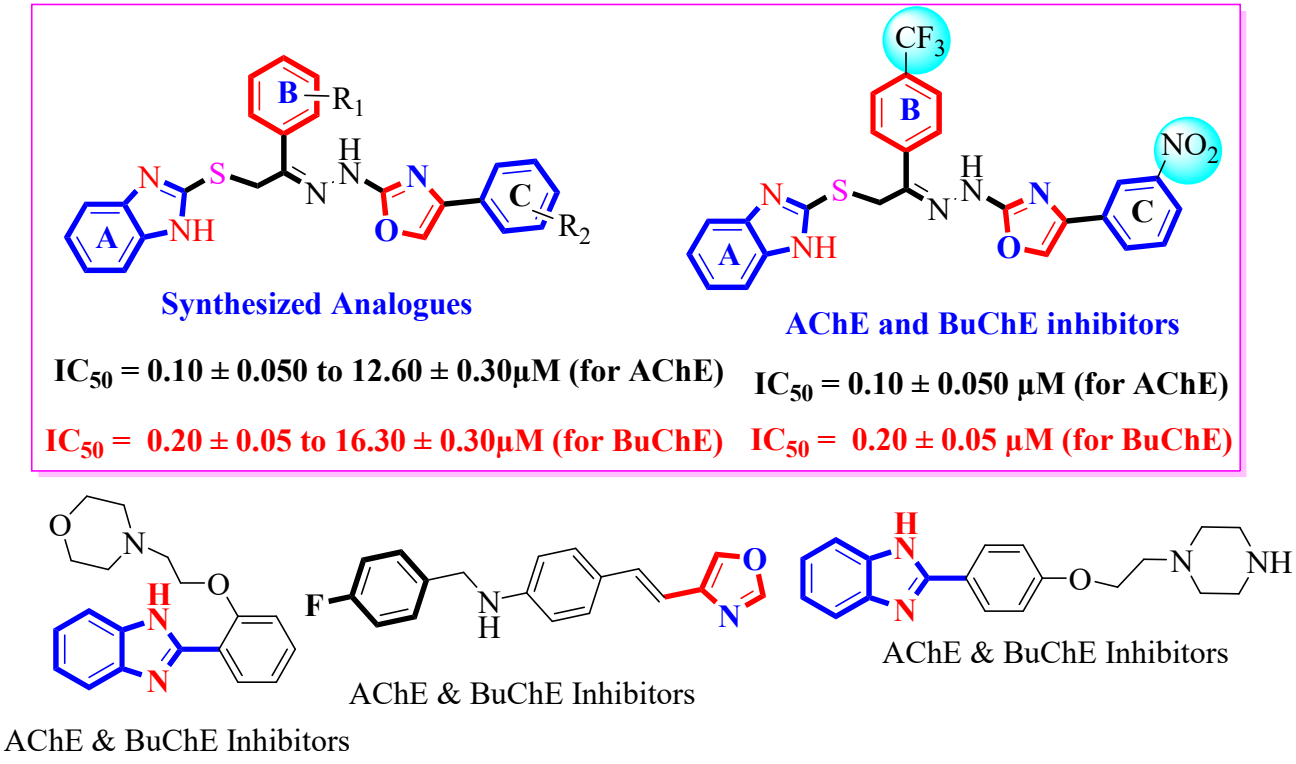


Figure 4. Rational of the current study.

2. Results and Discussion

2.1. Chemistry

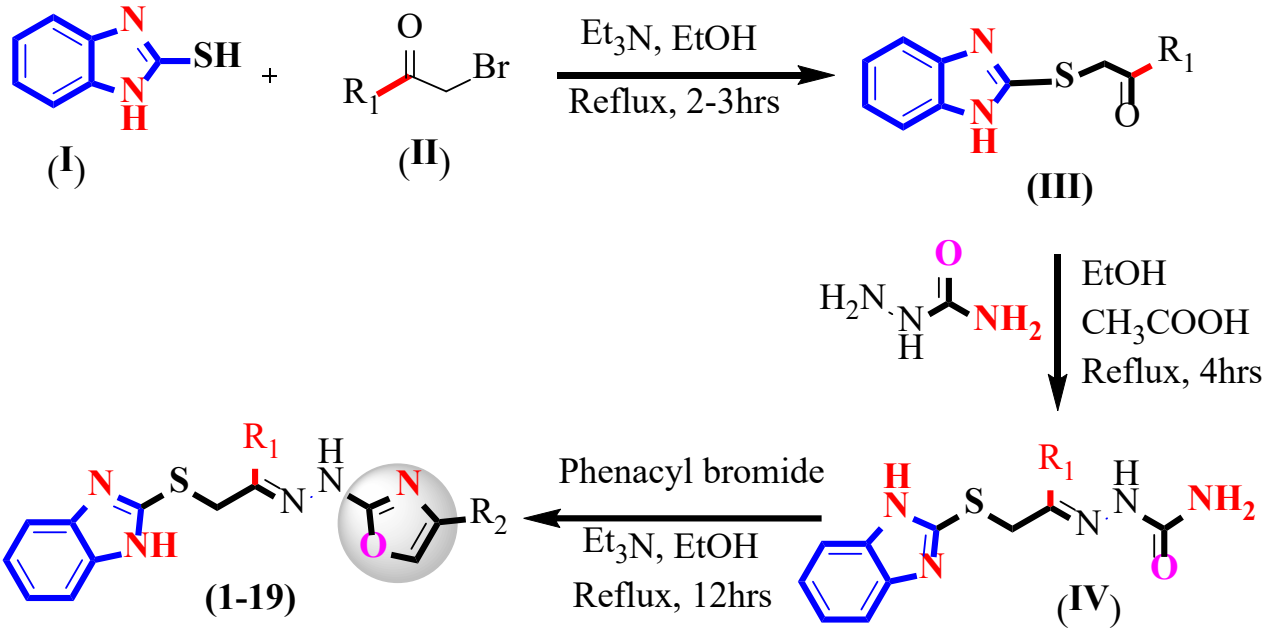
The synthesis of hybrid benzimidazole-based oxazole derivatives was completed in three steps:

First, the reaction mixture of 2-marcaptobenzimidazole (I, 1 mmol) and 2-bromoaceto phenone (II, 1 mmol) was mixed and refluxed for 2–3 h in ethanol (10 mL) in the presence of triethylamine as a catalyst to produce the first intermediate product (III) [32]. The second intermediate product (IV) was produced by treating the intermediate (III) and semicarbazide in equal amounts in ethanol (10 mL) and glacial acetic acid as catalysts and refluxing the mixture for around 4 h. After the reaction was complete, the mixture was cooled to room temperature, and the precipitate solid that was produced was filtered and washed with *n*-hexane. TLC plates had been used to keep tabs on the reaction's development. An equivalent quantity of intermediate (IV) underwent cyclization with stirring overnight with an equivalent amount of various substituted 2-bromoacetophenone in EtOH and Et_3N (catalyst) in order to produce the benzimidazole-oxazole hybrid compounds (**1**–**19**) in proper yield (Scheme 1). After cooling to 25 °C, the solvent was withdrawn, and the resulting solid residue was cleaned by washing with *n*-hexane before being re-crystallized from ethyl alcohol. Many spectroscopic techniques, including ^{13}C-NMR, ^{1}H-NMR, and HR-EIMS, were used to determine the structures of all freshly synthesized analogues.

2.2. In Vitro Acetylcholinesterase and Butyrylcholinesterase Inhibitory Activities

Hybrid analogues based on benzimidazole incorporating an oxazole skeleton were synthesised and then screened in vitro for their inhibitory activities against targeted AChE and BuChE enzymes as compared to donepezil as the standard drug. All synthesised benzimidazole-based oxazole analogues showed a varied range of inhibitory potentials against targeted AChE and BuChE enzymes, with IC50 values ranging from 0.10 ± 0.050 to 12.60 ± 0.30 µM (against AChE) and 0.20 ± 0.050 µM to 16.30 ± 0.30 µM (against BuChE) when compared to standard donepezil (IC50 = 2.16 ± 0.12 µM and 4.5 ± 0.11 µM, respectively (Table 1). Structure-activity relationship (SAR) studies have shown that inhibitory

potentials were greatly affected by changing either the position of substituent(s) or the nature of substituent(s) around both aryl parts; therefore, to better understand SAR studies, the synthesized analogues were split into various parts, including benzimidazole, oxazole, and aryl parts (R1 and R2), and it was further revealed from SAR studies that each part effectively contributed to inhibitory potentials, and any variation found on both aryl parts (R1 and R2, respectively) may result in different inhibitory potentials against targeted enzymes (Figure 5).



Scheme 1. Synthesis of benzimidazole-oxazole hybrid derivatives (**1**–**19**).

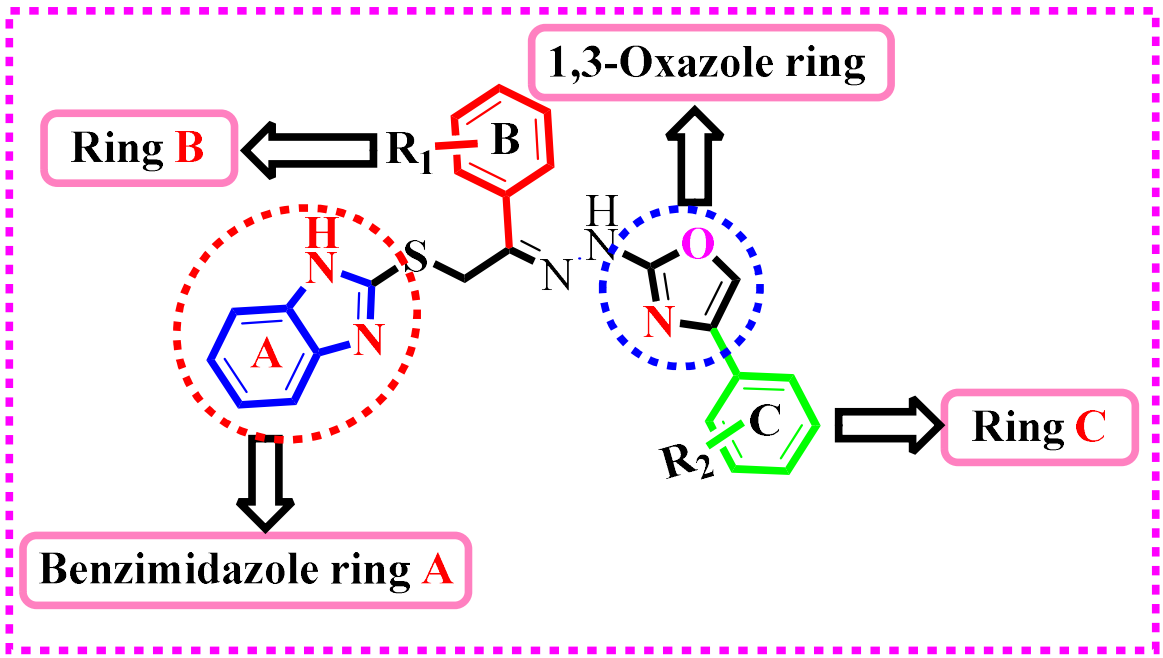


Figure 5. General structure of benzimidazole-oxazole hybrid derivatives (**1**–**19**).

Table 1. Different substituents, AChE and BuChE activities of benzimidazole-oxazole hybrid derivatives (**1**–**19**).

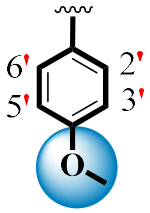
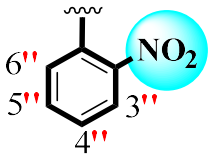
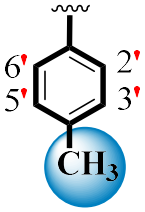
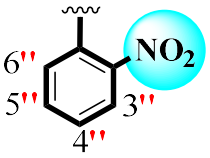
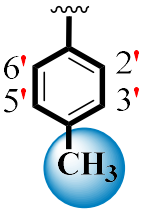
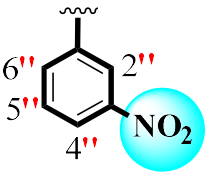
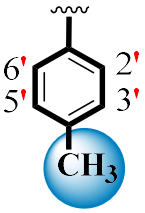
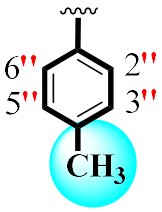
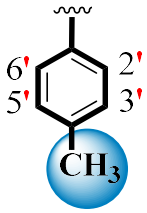
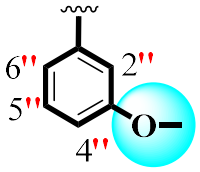
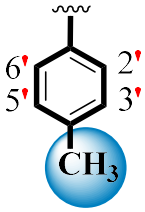
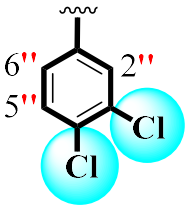
S.NO	R_1	R_2	AChE $IC_{50} \pm SEM$ [a] (μM)	BuChE $IC_{50} \pm SEM$ [a] (μM)
1			1.10 ± 0.10	1.80 ± 0.10
2			1.60 ± 0.010	1.90 ± 0.10
3			4.40 ± 0.10	5.80 ± 0.10
4			6.50 ± 0.20	8.30 ± 0.20
5			9.80 ± 0.20	11.50 ± 0.20
6			0.40 ± 0.05	1.10 ± 0.05

Table 1. *Cont.*

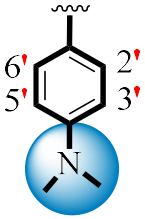
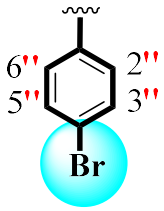
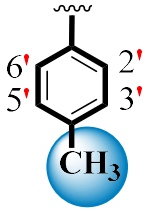
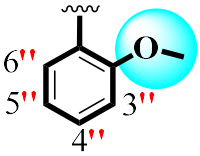
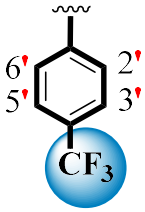
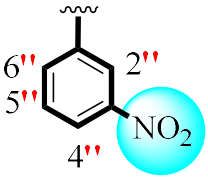
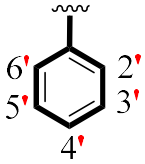
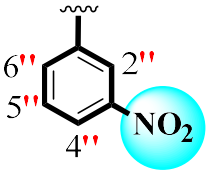
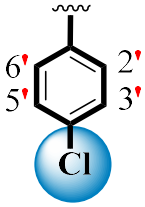
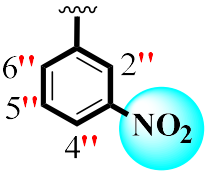
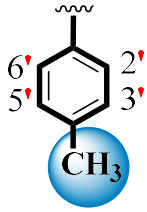
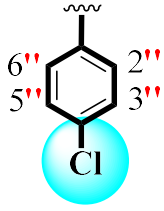
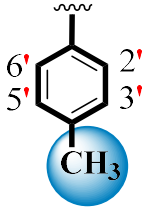
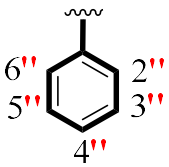
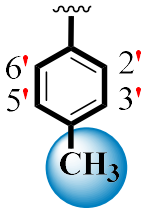
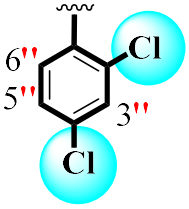
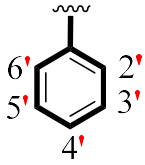
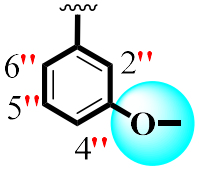
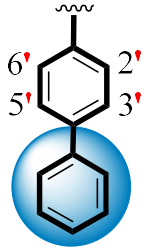
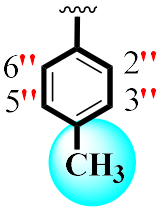
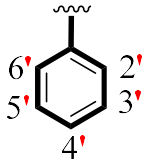
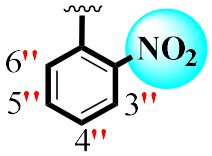
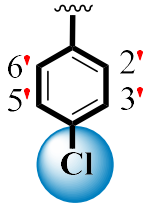
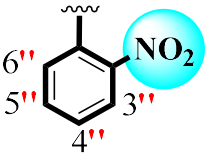
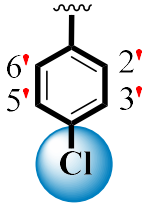
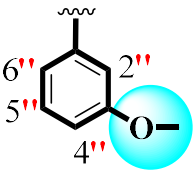
S.NO	R_1	R_2	AChE $IC_{50} \pm SEM$ [a] (μM)	BuChE $IC_{50} \pm SEM$ [a] (μM)
7			12.60 ± 0.30	16.30 ± 0.30
8			5.30 ± 0.20	7.20 ± 0.10
9			0.10 ± 0.050	0.20 ± 0.05
10			1.40 ± 0.10	2.10 ± 0.10
11			0.70 ± 0.050	1.20 ± 0.010
12			3.40 ± 0.10	5.70 ± 0.10
13			8.10 ± 0.10	9.70 ± 0.10

Table 1. *Cont.*

S.NO	R_1	R_2	AChE $IC_{50} \pm SEM$ [a] (μM)	BuChE $IC_{50} \pm SEM$ [a] (μM)
14			0.20 ± 0.050	0.30 ± 0.050
15			5.40 ± 0.10	7.20 ± 0.10
16			6.10 ± 0.10	9.30 ± 0.10
17			2.50 ± 0.10	3.50 ± 0.10
18			0.80 ± 0.10	1.70 ± 0.10
19			2.70 ± 0.20	3.70 ± 0.10
Standard drug Donepezil			2.16 ± 0.12	4.5 ± 0.11

[a] SEM is the standard error mean.

Structure Activity Relationship (SAR) for Acetylcholinesterase (AChE) and Butyrylcholinesterase (BuChE) Activities

Structure-activity relationships were performed on the basis of variety in different substitution patterns on both rings B and C, respectively. Derivatives 9 (IC50 = 0.10 ± 0.050 μM and 0.20 ± 0.050 μM), having a $-NO_2$ group at the 3-position on ring C and triflouromethyl substitution at the 4-position on ring B, and derivative 14, having dichloro substitution at

the 2- and 3-positions on ring C along with a methyl group at the para position on ring B, were identified as the first and second most potent inhibitors of AChE and BuChE enzymes among the synthesized derivatives.

Among the compounds with an unsubstituted ring B, derivative 10 (IC_{50} = 1.40 ± 0.10 μM and 2.10 ± 0.10 μM) had a nitro group at *meta* on ring C and derivative 17 (IC_{50} = 2.50 ± 0.10 μM and 3.50 ± 0.10μM) had a nitro group at *ortho* on ring C. The difference in the potentials of these derivatives may be due to the different positions of the nitro group on ring C.

By comparing the derivatives with a methyl group on ring B, derivative **2** (IC_{50} = 1.60 ± 0.10 μM and 1.90 ± 0.10 μM) had a $–NO_2$ group at the *ortho* position on ring C, derivative **3** (IC_{50} = 4.40 ± 0.10 μM and 5.80 ± 0.10 μM) had a $–NO_2$ group at the *meta* position on ring C, derivative **4** (IC_{50} = 9.80 ± 0.20 μM and 11.50 ± 0.20 μM) had methyl at the *para* position on ring C, derivative **5** (IC_{50} = 9.80 ± 0.20 μM and 11.50 ± 0.20 μM) had a methoxy group at the *meta* position on ring C, derivative **6** (IC_{50} = 0.40 ± 0.05 μM and 1.10 ± 0.05 μM) had dichloro substitutions at the *meta* and *para* positions on ring C, derivative **8** (IC_{50} = 5.30 ± 0.20 μM and 7.20 ± 0.10 μM) had a methoxy group at the *ortho* position on ring C, derivative **12** (IC_{50} = 0.40 ± 0.05 μM and 1.10 ± 0.05 μM) had a chloro group at the *para* position on ring C, and derivative **14** (IC_{50} = 0.20 ± 0.050 μM and 0.30 ± 0.050 μM) had dichloro substitutions at the *ortho* and *para* positions on ring C. The difference in the potentials of these entire derivatives may be due to the different nature, number, and position of the substituents on ring C.

Among the derivatives having a chloro group on ring B, compound **11** (IC_{50} = 0.70 ± 0.50 μM and 1.20 ± 0.010 μM) had a NO_2 group at the *meta* position on ring C, **18** (IC_{50} = 0.80 ± 0.10 μM and 1.70 ± 0.10 μM) had a nitro group at the *ortho* position on ring C, and **19** (IC_{50} = 2.70 ± 0.20 μM and 1.10 ± 0.05 μM) had an OCH_3 group at the meta position on ring C, correspondingly. The difference in the inhibitory potentials of these derivatives may be due to the different nature, number, and position of the substituents on ring C.

Overall, it was also observed that the variation in number, nature, and position of certain groups at particular positions on rings B and C greatly affects the inhibitory potentials of the synthesized derivatives. Therefore, a molecular docking study was performed to understand the binding interaction of the most potent derivatives with the active site of enzymes.

2.3. Molecular Docking Study

A molecular docking study was performed on the most active benzimidazole-oxazole analogues (9, 14, and 6) in order to elucidate the in vitro study. Subsequently, all these active analogues showed a well-fitting binding mode with different binding affinities and correlated well with the in vitro studies. All of the active compounds, 9, 14, and 6, have similar and related chemistry, with slight modifications at different positions. These different functional moieties showed wide differences in their interactions with the active pocket of the targeted enzyme. Compound 9 showed maximum interactions with the active sites of both targeted AChE and BuChE enzymes and was found to be the most effective, and this was similar in the in vitro study. The details of the interactions are given in Table 2. It was also found that not only does the direct attachment of the electron-withdrawing group ($–NO_2$) cause good activity, but the indirect attachment of the electron-withdrawing $–F_3$ moiety in the form of $–CF_3$ is also important, which in turn attaches the ring of the analogue. The better interactions, activity, and docking score of analogue 9 were mainly due to this reason. The electron-withdrawing $–NO_2$ and $–CF_3$ groups withdraw electronic density from the extended benzene ring, making the benzene ring more electrophilic; hence, the extended benzene ring remains electron-deficient, which further regains stability by forming pi-cation interactions with the active site of the targeted enzyme. From docking analysis, it was found that not only do electron-withdrawing groups such as $–NO_2$ and $–CF_3$ groups enhance the activity by making the benzene ring cationic, but they also enhance the enzymatic activity through the sidewise involvement of the oxygen of $–NO_2$ and –F in

hydrogen bonding and halogen (fluorine) with the active sites of both targeted enzymes. The presence of the $-NO_2$ functional group is more effective in its *meta*-position; therefore, compound 9 has very good activity and interactions, as shown in Table 2. Compound 14, which holds electron-withdrawing di-Cl moieties at the 2,4-position of ring C and the para-methyl substation on ring B, was proven to be the second most active analogue and adopted several significant interactions with the active sites of both targeted AChE and BuChE (Table 2). Changing the position of di-Cl moieties around ring C, as in the case of compound **6**, resulted in different enzymatic activities and hence different interactions with the active sites of both targeted AChE and BuChE enzymes (Figures 6–11, Table 2).

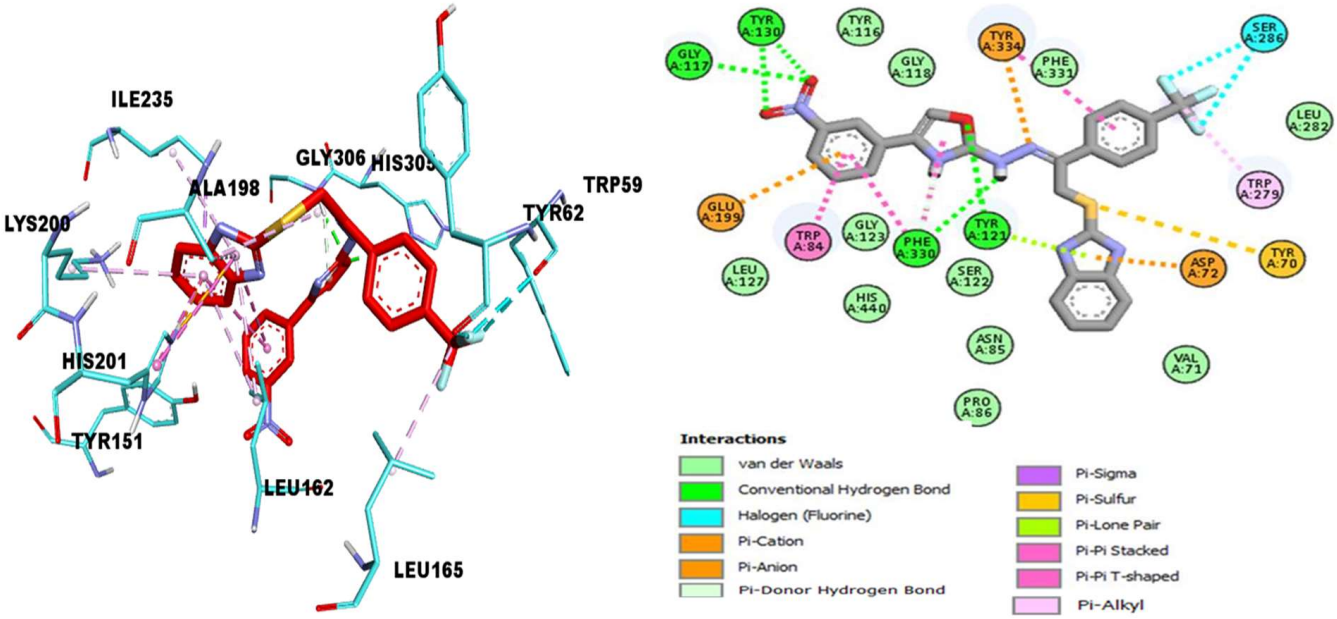


Figure 6. The protein-ligand interaction (PLI) profile of compound **9** against the AChE enzyme and its 3D (**left**) and 2D (**right**) diagrams.

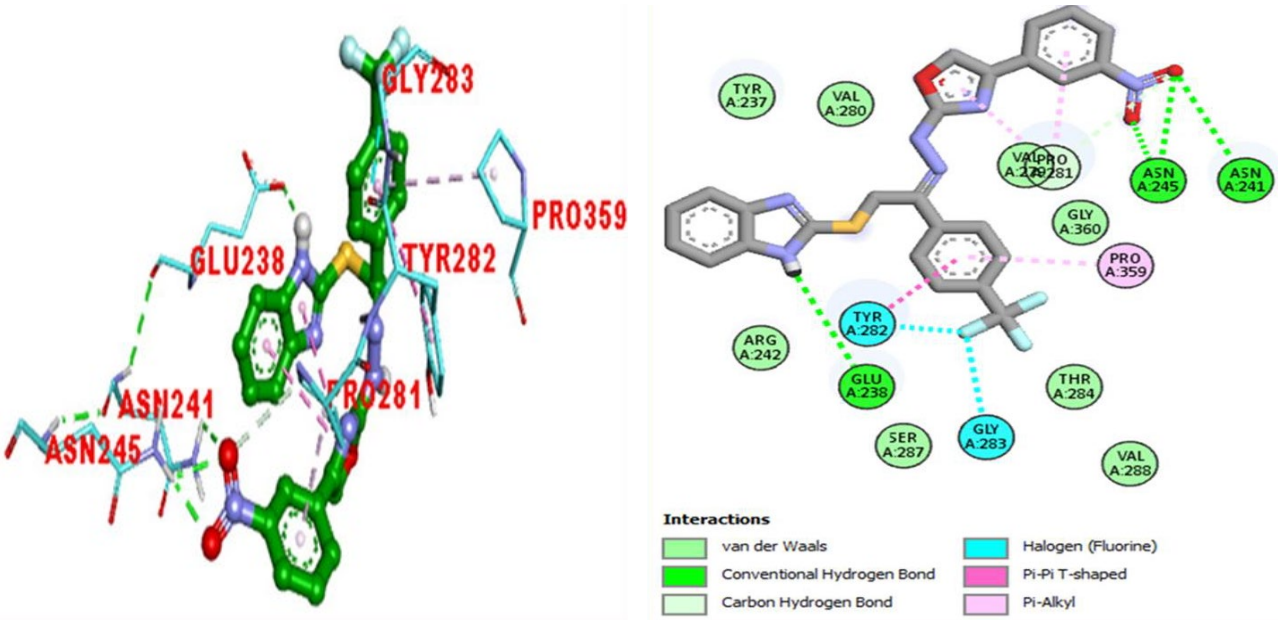


Figure 7. The protein-ligand interaction (PLI) profile of compound **9** against the BuChE enzyme and its 3D (**left**) and 2D (**right**) diagrams.

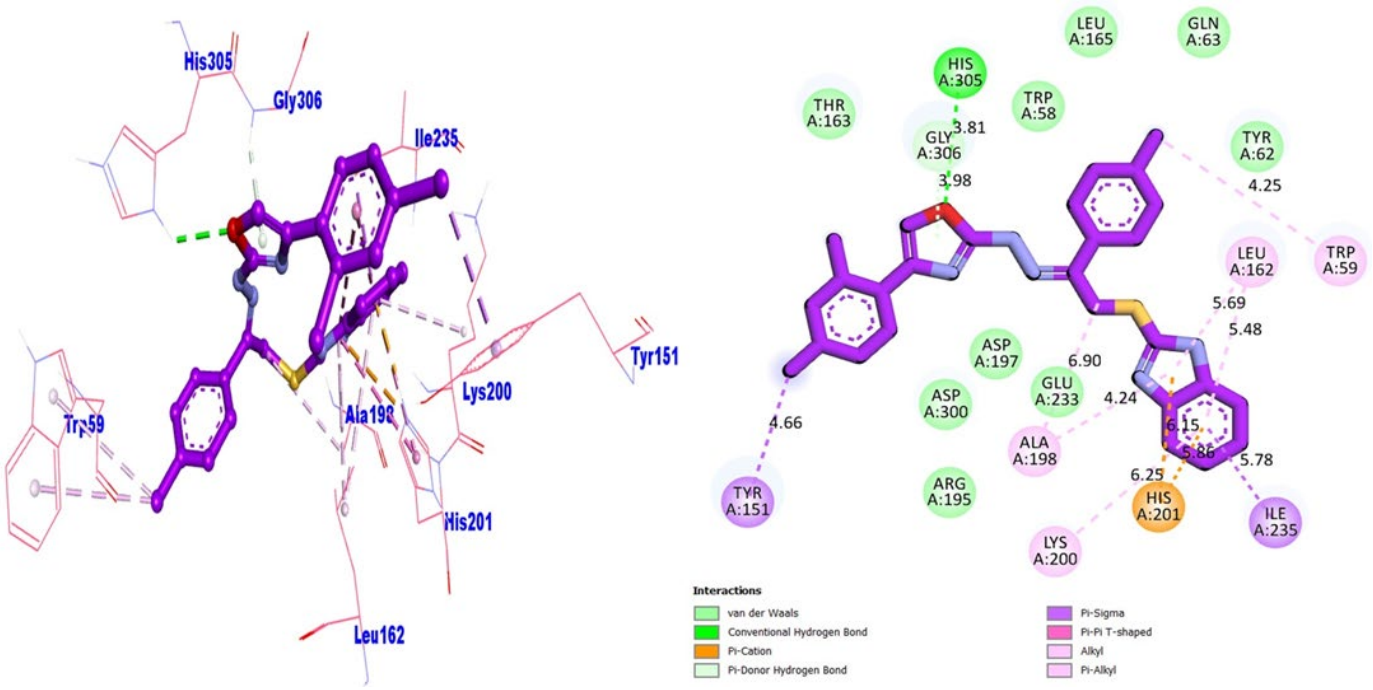


Figure 8. Protein-ligand interaction profile (PLI) of the second most active compound **14** against the AChE enzyme and its 3D (**left**) and 2D (**right**) diagrams.

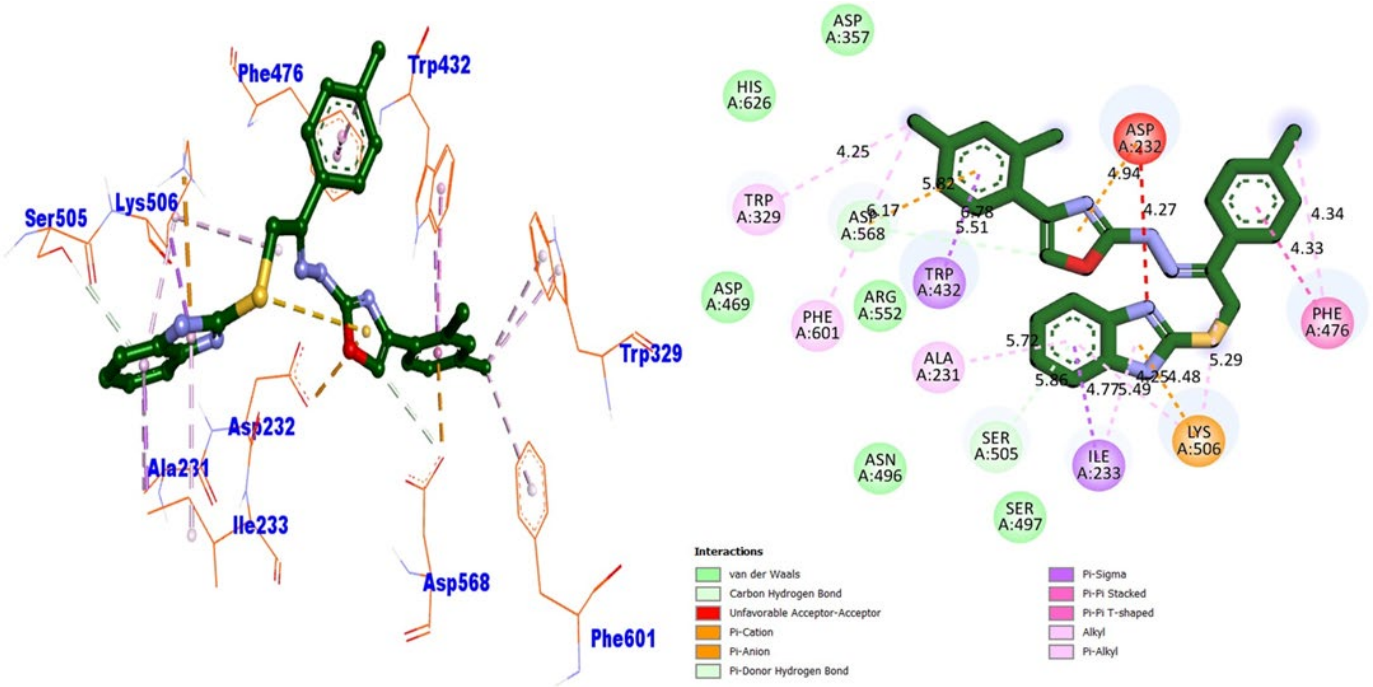


Figure 9. Protein-ligand interaction profile (PLI) of the second most active compound **14** against the BuChE enzyme and its 3D (**left**) and 2D (**right**) diagrams.

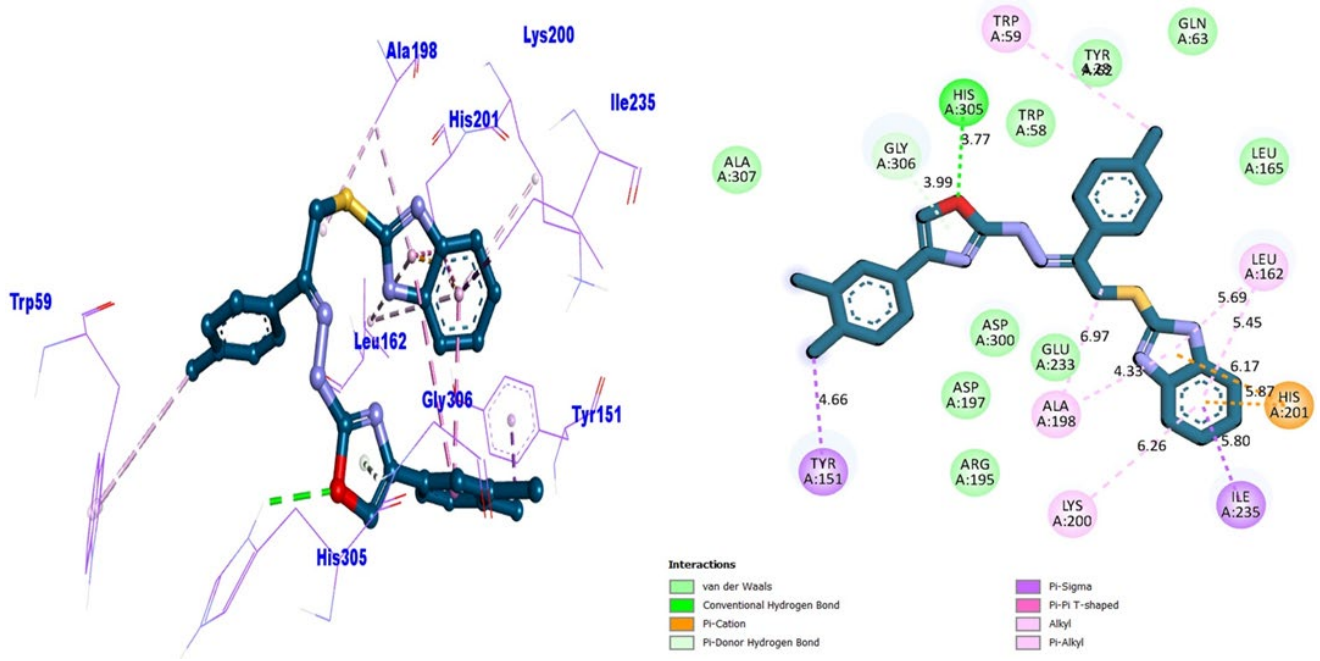


Figure 10. Protein-ligand interaction profile (PLI) of the third most active compound **6** against the AChE enzyme and its 3D (**left**) and 2D (**right**) diagrams.

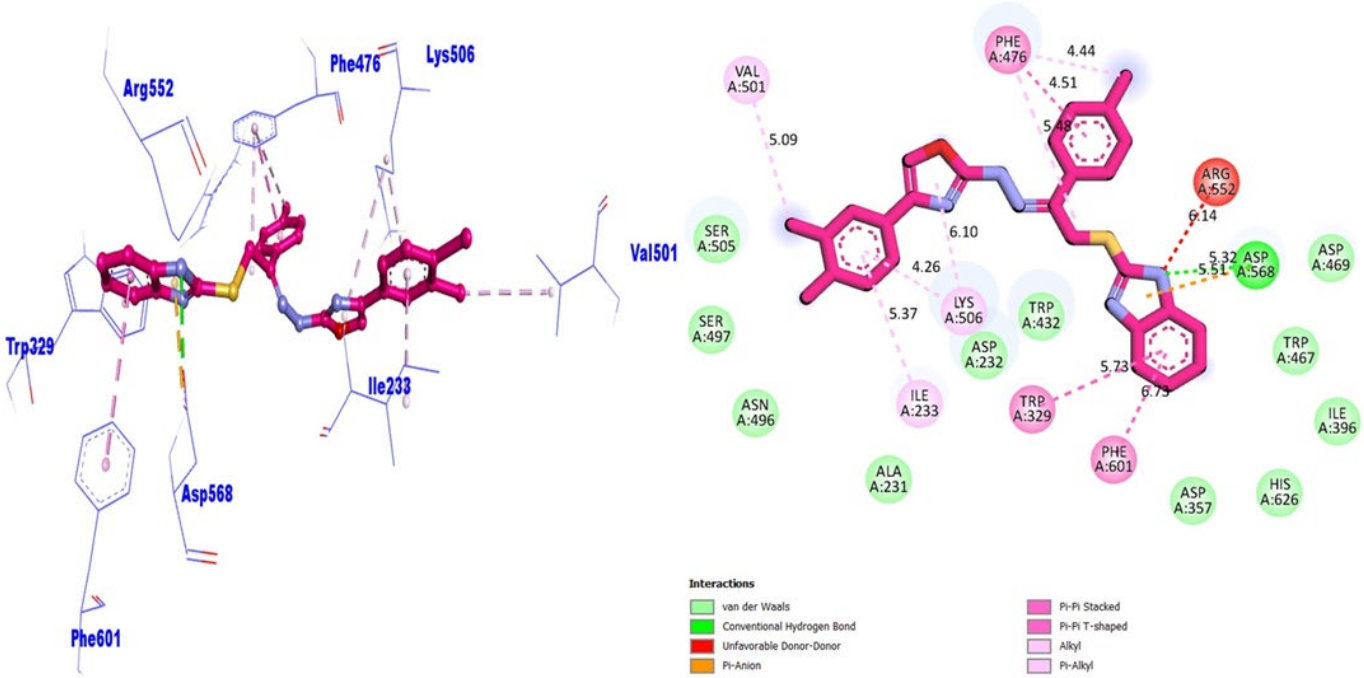


Figure 11. Protein-ligand interaction profile (PLI) of the third most active compound **6** against the BuChE enzyme and its 3D (**left**) and 2D (**right**) diagrams.

Table 2. The different types of interactions between active analogues (**9**, **14**, and **6**) and interactive residues of amino acids of the targeted AChE and BuChE enzymes with varied distances.

Active Analogues	Targeted Enzymes	Receptors	Interactions	Binding Affinities (kJ/mol)
Analogue-**9**	AChE	GLY-117	HB	−12.37
		TYR-130	HB	
		GLU-198	π-cation	
		TRP-84	π-π T-shaped	
		PHE-330	π-π T-shaped, π-alkyl and HB	
		TYR-221	HB and Carbon HB	
		ASP-72	π-anion	
		TYR-70	π-sulphur	
		TYR-334	π-π stacked and π-anion	
		TRP-279	π-alkyl	
		SER-286	Halogen (fluorine)	
	BuChE	GLU-238	HB	−11.97
		ASN-245	HB	
		ASN-241	HB	
		PRO-281	π-alkyl	
		VAL-229	π-alkyl	
		PRO-359	π-alkyl	
		TYR-282	π-π stacked and halogen (fluorine)	
		GLY-283	halogen (fluorine)	
Analogue-**14**	AChE	TYR-151	π-sigma	−11.17
		HIS-305	HB	
		ALA-198	π-alkyl	
		LYS-200	π-alkyl	
		ILE-235	π-sigma	
		LEU-162	π-alkyl	
		TRP-59	π-alkyl	
		HIS-201	π-cation	
	BuChE	TRP-329	π-alkyl	−10.87
		PHE-601	π-alkyl	
		ASP-568	π-cation	
		TRP-432	π-sigma	
		ASP-568	Carbon HB	
		ASP-232	π-cation	
		ALA-231	π-alkyl	
		SER-505	Carbon HB	
		ILE-233	π-sigma and π-π T shaped	
		LYS-506	π-anion and π-π T-shaped	
		LYS-506	π-alkyl	
		PHE-476	π-π T-shaped and π-alkyl	

Table 2. *Cont.*

Active Analogues	Targeted Enzymes	Receptors	Interactions	Binding Affinities (kJ/mol)
Analogue-**6**	AChE	TYR-151	π-sigma	−10.12
		GLY-306	Carbon HB	
		HIS-305	HB	
		ALA-198	π-alkyl	
		LYS-200	π-alkyl	
		ILE-235	π-sigma	
		HIS-201	π-cation	
		LEU-162	π-alkyl	
		TRP-59	π-alkyl	
	BuChE	VAL-501	π-alkyl	−9.76
		ILE-233	π-alkyl	
		LYS-506	π-alkyl	
		TRP-329	π-π T-shaped	
		PHE-601	π-π T-shaped	
		ASP-568	π-anion	
		ASP-568	HB	
		PHE-476	π-π stacked and π-alkyl	

2.4. ADMET Analysis

ADMET analysis describes the different properties of the subjected ligand, such as log Kp, Lipinski, Ghose, Veber, Egan, Muegge, Bioavailability, PAINS, and Brenk, etc. (Figures 12–14).

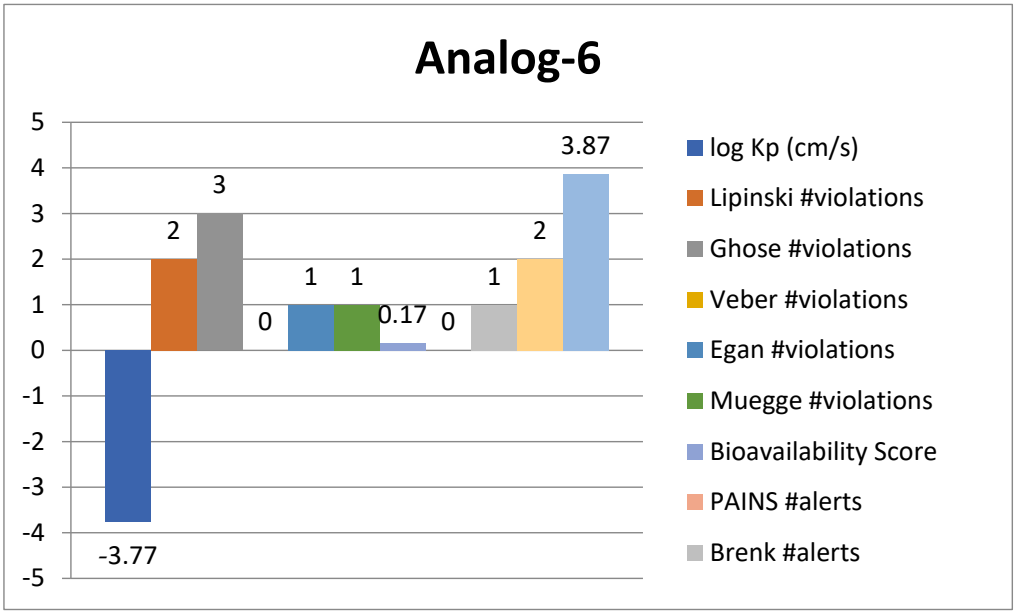


Figure 12. Representation of the ADMET analysis of analog-**6**.

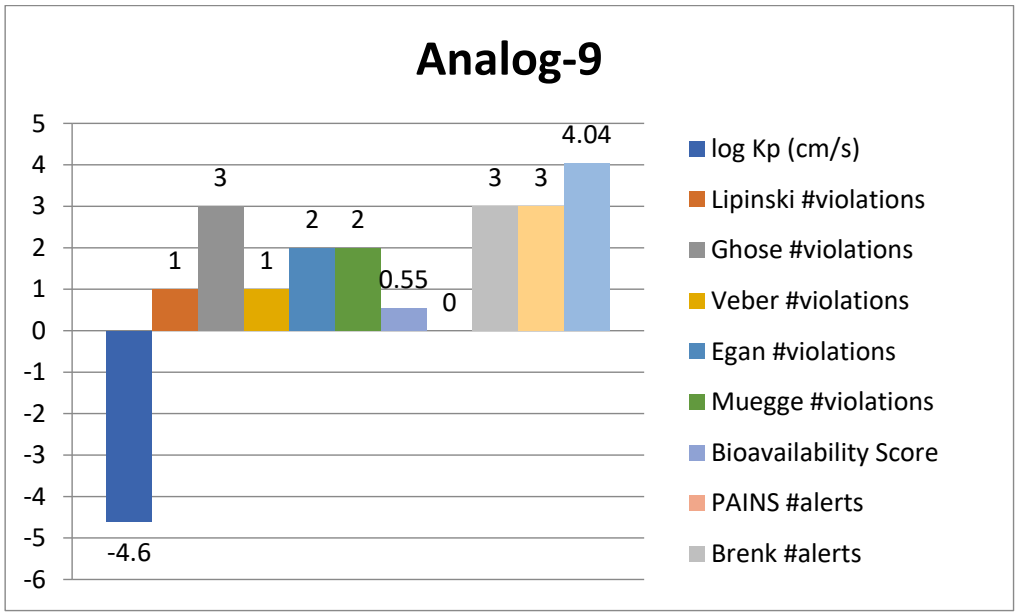


Figure 13. Representation of the ADMET analysis of analog-**9**.

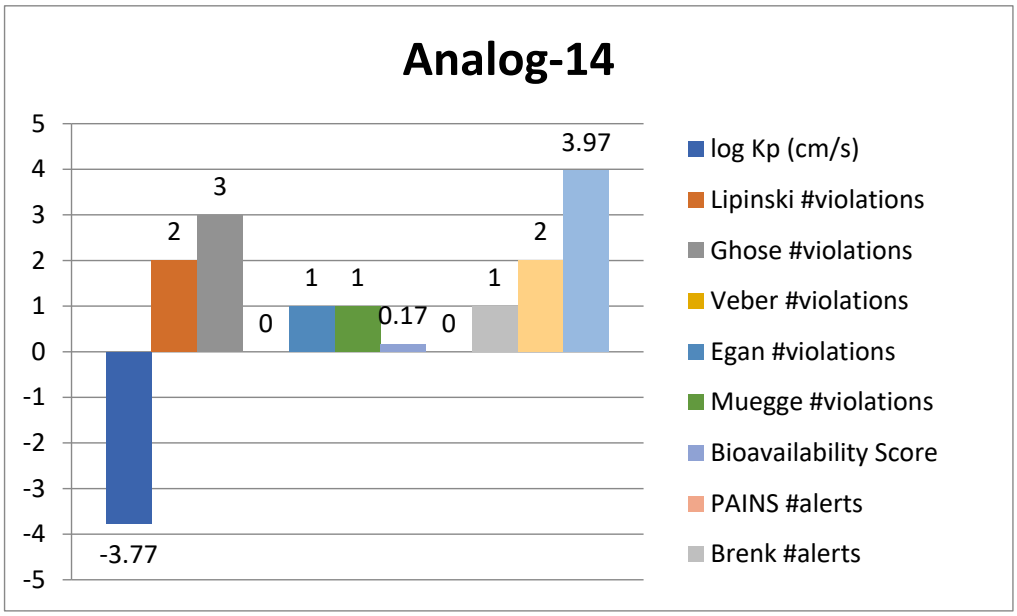


Figure 14. Representation of the ADMET analysis of analog-**14**.

3. Experiment

*3.1. General Procedure for the Synthesis of Benzimidazole-Oxazole Hybrid Derivatives (**1**–**19**)*

2-Marcaptobenzimidazole (I, 1 mmol) and 2-bromoacetophenone (II, 1 mmol) were mixed and refluxed for 2–3 h in ethanol (10 mL) in the presence of triethylamine to produce the first intermediate product (III) [32]. The second intermediate product (IV) was produced by treating the intermediate (III) and semicarbazide in equal amounts in ethanol (10 mL) and glacial acetic acid as catalysts and refluxing the mixture for around 4 h. After the reaction was complete, the mixture was cooled to room temperature, and the precipitate solid that was produced was filtered and washed with *n*-hexane. TLC plates were used to check the reaction's development. An equivalent quantity of intermediate (IV) underwent cyclization with stirring overnight with an equivalent amount of various substituted 2-bromoacetophenone in EtOH and Et_3N (catalyst) in order to produce the benzimidazole-

oxazole hybrid compounds (**1**–**19**) at proper yield. After cooling to 25 °C, the solvent was withdrawn, and the resulting solid residue was cleaned by washing with *n*-hexane before being re-crystallized from ethyl alcohol.

3.2. Spectral Analysis

Spectra of some compounds are provided as Supplementary Materials.

3.2.1. (E)-2-(2-(2-((1H-Benzo[d]imidazol-2-yl)thio)-1-(4-methoxyphenyl)ethylidene)hydrazinyl)-4-(2-nitrophenyl)oxazole (1)

Yield: 69%; Rf value 0.59 (7:3 n-hex: EtOAc); ^{1} H NMR (600 MHz, DMSO-d_6): δ12.75 (s, 1H, -NH), 10.67 (s, 1H, -NH), 8.21 (dd, $J_{(6'', 5'')}$ = 8.0Hz, $J_{(6'', 4'')}$ = 2.4Hz, 1H, H-6″), 8.13 (d, $J_{(3'', 4'')}$ = 7.8 Hz, 1H, H-3″), 8.02 (d, $J_{(2', 3'/ 6', 5')}$ = 8.6Hz, 2H, H-2′/H-6′), 7.96 (s, 1H, oxazole-H), 7.93–7.86 (m, 1H, H-5″), 7.82 (t, $J_{(4''/5'', 3'')}$ = 9.0Hz, 1H, H-4″), 7.65 (m, 2H, H-4/H-7), 7.34 (m, 2H, H-5/H-6), 7.13 (d, $J_{(3', 2'/5', 6')}$ = 8.0 Hz, 2H, H-3′/H-5′), 3.98 (s, 2H, S-CH_2), 3.85 (s, 3H, -OCH_3); ^{13}C-NMR (150 MHz, DMSO-d6): δ 163.2, 157.2, 152.2, 149.8, 148.7, 141.7, 141.5, 140.5, 140.3, 136.3, 133.6, 130.6, 129.0, 129.0, 126.6, 126.2, 125.4, 124.6, 124.3, 116.8, 116.6, 114.7, 114.7, 56.1, 39.1.; HR-MS (ESI): (*m*/*z*) [M + H]$^+$ calculated for $C_{25}H_{21}N_6O_4S$ 501.1342, found 501.1351.

3.2.2. (*E*)-2-(2-(2-((1H-Benzo[d]imidazol-2-yl)thio)-1-(*p*-tolyl)ethylidene)hydrazinyl)-4-(2-nitrophenyl)oxazole (**2**)

Yield: 67%; Rf value 0.61 (7:3 n-hex: EtOAc); ^{1} H NMR (600 MHz, DMSO-d_6): δ13.34 (s, 1H, -NH), 11.25 (s, 1H, -NH), 7.79 (dd, $J_{(6'', 5'')}$ = 8.4 Hz, $J_{(6'', 4'')}$ = 2.0 Hz, 1H, H-6″), 7.72 (d, $J_{(3'', 4'')}$ = 7.9 Hz, 1H, H-3″), 7.53 (s, 1H, oxazole-H), 7.36–7.33 (m, 1H, H-5″), 7.29 (d, $J_{(2', 3'/ 6', 5')}$ = 7.5 Hz, 2H, H-2′/H-6′), 7.24 (t, $J_{(4''/5'', 3'')}$ = 9.2 Hz, 1H, H-4″), 7.22 (d, $J_{(3', 2'/5', 6')}$ = 6.7 Hz, 2H, H-3′/H-5′), 7.11–7.08 (m, 2H, H-4/H-7), 6.98–6.96 (m, 2H, H-5/H-6), 2.50 (s, 2H, S-CH_2), 1.22 (s, 3H, -CH_3); ^{13}C-NMR (150 MHz, DMSO-d6): δ 156.6, 151.6, 149.5, 148.1, 141.9, 141.1, 140.9, 139.9, 139.7, 136.0, 133.3, 132.4, 130.5, 130.3, 130.3, 128.2, 128.2, 125.9, 125.1, 124.0, 123.7, 116.2, 116.0, 38.5, 22.5.; HR-MS (ESI): (*m*/*z*) [M + H]$^+$ calculated for $C_{25}H_{21}N_6O_3S$ 485.1393, found 485.1401.

3.2.3. (*E*)-2-(2-(2-((1H-Benzo[d]imidazol-2-yl)thio)-1-(*p*-tolyl)ethylidene)hydrazinyl)-4-(3-nitrophenyl)oxazole (**3**)

Yield: 73%; Rf value 0.57 (7:3 n-hex: EtOAc); ^{1} H NMR (600 MHz, DMSO-d_6): δ12.69 (s, 1H, -NH), 10.61 (s, 1H, -NH), 8.53 (t, $J_{(2''/4'', 6'')}$ = 2.6 Hz, 1H, H-2″), 8.33 (d, $J_{(6'', 5'')}$ = 6.6 Hz, 1H, H-6″), 8.22–8.16 (m, 1H, H-4″), 7.89 (t, $J_{(5''/4'', 6'')}$ = 7.8 Hz, 1H, H-5″), 7.84 (s, 1H, oxazole-H), 7.77 (d, $J_{(2', 3'/ 6', 5')}$ = 8.2 Hz, 2H, H-2′/H-6′), 7.59–7.51 (m, 2H, H-4/H-7), 7.34 (d, $J_{(3', 2'/5', 6')}$ = 7.5 Hz, 2H, H-3′/H-5′), 7.28–7.19 (m, 2H, H-5/H-6), 3.92 (s, 2H, S-CH_2), 2.49 (s, 3H, -CH_3).; ^{13}C-NMR (150 MHz, DMSO-d6): δ 157.1, 152.1, 149.0, 148.6, 142.4, 141.6, 141.4, 140.4, 140.2, 134.5, 134.2, 132.7, 131.2, 130.8, 130.8, 128.7, 128.7, 124.7, 124.5, 124.2, 123.3, 116.7, 116.5, 39.0, 23.0.; HR-MS (ESI): (*m*/*z*) [M + H]$^+$ calculated for $C_{25}H_{21}N_6O_3S$ 485.1393, found 485.1401.

3.2.4. (*E*)-2-(2-(2-((1H-Benzo[d]imidazol-2-yl)thio)-1-(*p*-tolyl)ethylidene)hydrazinyl)-4-(*p*-tolyl)oxazole (**4**)

Yield: 74%; Rf value 0.63 (7:3 n-hex: EtOAc); ^{1} H NMR (600 MHz, DMSO-d_6): δ12.66 (s, 1H, -NH), 10.58 (s, 1H, -NH), 7.83 (d, $J_{(2', 3'/ 6', 5')}$ = 6.6 Hz, 2H, H-2′/H-6′), 7.81 (s, 1H, oxazole-H), 7.69 (d, $J_{(2'', 3''/ 6'', 5'')}$ = 7.9 Hz, 2H, H-2″/H-6″), 7.56–7.48 (m, 2H, H-4/H-7), 7.40 (d, $J_{(3', 2'/5', 6')}$ = 7.0 Hz, 2H, H-3′/H-5′), 7.29–7.22 (m, 2H, H-5/H-6), 7.23 (d, $J_{(3'', 2''/5'', 6'')}$ = 8.5 Hz, 2H, H-3″/H-5″), 3.89 (s, 2H, S-CH_2), 2.44 (s, 3H, -CH_3), 2.54 (s, 3H, -CH_3).; ^{13}C-NMR (150 MHz, DMSO-d6): δ 165.9, 164.3, 162.7, 160.3,159.4, 157.07, 135.9, 131.0, 131.0, 130.6, 130.6, 130.2, 130.1,129.4, 129.3, 128.6, 128.3, 128.2, 127.7, 120.6, 116.1, 115.9, 115.8,

115.8, 115.7, 64.8, 40.0, 21.0, 15.1.; HR-MS (ESI): (*m*/*z*) $[M + H]^+$ calculated for $C_{26}H_{24}N_5OS$ 454.1698, found 454.1707.

3.2.5. (*E*)-2-(2-(2-((1H-Benzo[d]imidazol-2-yl)thio)-1-(*p*-tolyl)ethylidene)hydrazinyl)-4-(3-methoxyphenyl)oxazole (**5**)

Yield: 76%; Rf value 0.56 (7:3 n-hex: EtOAc); ^{1} H NMR (600 MHz, DMSO-d_6): δ12.80 (s, 1H, -NH), 10.72 (s, 1H, -NH), 7.95 (s, 1H, oxazole-H), 7.76–7.69 (m, 2H, H-4/H-7), 7.65 (d, $J_{(2', 3'/ 6', 5')}$ = 9.4 Hz, 2H, H-2′/H-6′), 7.60–7.54 (m, 1H, H-6″), 7.52 (dd, $J_{(5'', 4'')}$ = 9.2 Hz, $J_{(5'', 6'')}$ = 9.0 Hz, 1H, H-5″), 7.44 (t, $J_{(2''/4'', 6'')}$ = 2.8 Hz, 1H, H-2″), 7.39 (m, 2H, H-5/H-6), 7.18 (d, $J_{(3', 2'/5', 6')}$ = 8.6 Hz, 2H, H-3′/H-5′), 7.14 (d, $J_{(4'', 5'')}$ = 8.5 Hz, 1H, H-4″), 4.04 (s, 2H, S-CH_2), 3.91 (s, 3H, -OCH_3), 2.32 (s, 3H, -CH_3).; ^{13}C-NMR (150 MHz, DMSO-d6): δ 161.7, 155.2, 150.2, 146.7, 142.1, 139.7, 139.5, 138.5, 138.3, 134.6, 132.4, 130.8, 130.5, 130.5, 128.4, 128.4, 122.6, 122.3, 120.4, 114.9, 114.8, 114.6, 114.2, 56.4, 37.1, 22.7; HR-MS (ESI): (*m*/*z*) $[M + H]^+$ calculated for $C_{26}H_{24}N_5O_2S$ 470.1645, found 470.1656.

3.2.6. (*E*)-2-(2-(2-((1H-Benzo[d]imidazol-2-yl)thio)-1-(*p*-tolyl)ethylidene)hydrazinyl)-4-(3,4-dichlorophenyl)oxazole (**6**)

Yield: 67%; Rf value 0.58 (7:3 n-hex: EtOAc); ^{1} H NMR (600 MHz, DMSO-d_6): δ12.80 (s, 1H, -NH), 10.72 (s, 1H, -NH), 8.09 (d, $J_{(2'', 6'')}$ = 2.8 Hz, 1H, H-2″), 7.98 (dd, $J_{(6'', 5'')}$ = 8.8 Hz, $J_{(6'', 2'')}$ = 1.7 Hz, 1H, H-6″), 7.93 (s, 1H, oxazole-H), 7.81 (d, $J_{(2', 3'/ 6', 5')}$ = 8.4 Hz, 2H, H-2′/H-6′), 7.75–7.70 (m, 2H, H-4/H-7), 7.65 (d, $J_{(5'', 6'')}$ =7.5 Hz, 1H, H-5″), 7.45–7.39 (m, 2H, H-5/H-6), 7.33 (d, $J_{(3', 2'/5', 6')}$ = 9.0 Hz, 2H, H-3′/H-5′), 4.04 (s, 2H, S-CH_2), 2.48 (s, 3H, -CH_3).; ^{13}C-NMR (150 MHz, DMSO-d6): δ 157.6, 152.6, 149.1, 142.4, 142.1, 141.9, 140.9, 140.7, 134.4, 133.7, 133.5, 132.5, 131.7, 130.6, 130.6, 129.8, 128.5, 128.5, 128.0, 125.0, 124.7, 117.2, 117.0, 39.5, 22.8.; HR-MS (ESI): (*m*/*z*) $[M + H]^+$ calculated for $C_{25}H_{20}Cl_2N_5OS$ 508.0763, found 508.0771.

3.2.7. (*E*)-4-(2-((1H-Benzo[d]imidazol-2-yl)thio)-1-(2-(4-(4-bromophenyl)oxazol-2-yl)hydrazono)ethyl)-*N*,*N*-dimethylaniline (**7**)

Yield: 65%; Rf value 0.53 (7:3 n-hex: EtOAc); ^{1} H NMR (600 MHz, DMSO-d_6): δ13.33 (s, 1H, -NH), 11.26 (s, 1H, -NH), 7.84 (s, 1H, oxazole-H), 7.77 (d, $J_{(2'', 3''/ 6'', 5'')}$ = 7.9 Hz, 2H, H-2″/H-6″), 7.55–7.53 (m, 2H, H-4/H-7), 7.45 (d, $J_{(3'', 2''/5'', 6'')}$ = 7.5 Hz, 2H, H-3″/H-5″), 7.36 (d, $J_{(2', 3'/ 6', 5')}$ = 8.6 Hz, 2H, H-2′/H-6′), 7.33 (m, 2H, H-5/H-6), 7.10–6.84 (d, $J_{(3', 2'/5', 6')}$ = 9.4 Hz, 2H, H-3′/H-5′), 3.81 (s, 6H, -$N(CH_3)_2$), 3.51 (s, 2H, S-CH_2); ^{13}C-NMR (150 MHz, DMSO-d6): δ 155.3, 150.3, 146.8, 142.6, 139.8, 139.6, 138.6, 138.4, 132.9, 132.5, 132.5, 131.0, 131.0, 130.1, 128.9, 128.9, 128.7, 128.7, 123.6, 122.7, 122.4, 114.9, 114.7, 37.2, 23.2.; HR-MS (ESI): (*m*/*z*) $[M + H]^+$ calculated for $C_{26}H_{24}BrN_6OS$ 547.0911, found 547.0908.

3.2.8. (*E*)-2-(2-(2-((1H-Benzo[d]imidazol-2-yl)thio)-1-(*p*-tolyl)ethylidene)hydrazinyl)-4-(2-methoxyphenyl)oxazole (**8**)

Yield: 78%; Rf value 0.56 (7:3 n-hex: EtOAc); ^{1} H NMR (600 MHz, DMSO-d_6): δ12.64 (s, 1H, -NH), 10.56 (s, 1H, -NH), 8.33 (d, $J_{(6'', 5'')}$ = 7.0 Hz, 1H, H-6″), 7.83 (d, $J_{(2', 3'/ 6', 5')}$ = 7.7 Hz, 2H, H-2′/H-6′), 7.75 (s, 1H, oxazole-H), 7.55 (m, 2H, H-4/H-7), 7.52 (t, $J_{(4''/5'', 3'')}$ = 9.0 Hz, 1H, H-4″), 7.47 (dd, $J_{(5'', 4'')}$ = 8.8 Hz, $J_{(5'', 6'')}$ = 7.9 Hz, 1H, H-5″), 7.37 (d, $J_{(3', 2'/5', 6')}$ = 6.8 Hz, 2H, H-3′/H-5′), 7.26 (d, $J_{(3'', 4'')}$ = 8.7 Hz, 1H, H-3″), 7.23 (m, 2H, H-5/H-6), 3.87 (s, 2H, S-CH_2), 3.82 (s, 3H, -OCH_3), 2.53 (s, 3H, -CH_3).; ^{13}C-NMR (150 MHz, DMSO-d6): δ 158.3, 156.9, 151.9, 148.4, 141.4, 141.2, 140.2, 142.0, 140.0, 132.5, 132.1, 130.7, 130.4, 130.4, 128.3, 128.3, 124.3, 124.0, 122.5, 119.9, 116.5, 116.3, 112.1, 57.1, 38.8, 22.6.; HR-MS (ESI): (*m*/*z*) $[M + H]^+$ calculated for $C_{26}H_{24}N_5O_2S$ 470.1645, found 470.1656.

3.2.9. (*E*)-4-(2-(2-(2-((1H-Benzo[d]imidazol-2-yl)thio)-1-(*p*-tolyl)ethylidene)hydrazinyl) Oxa-zol-4-yl)phenol (**9**)

Yield: 70%; Rf value 0.64 (7:3 n-hex: EtOAc); ^{1} H NMR (600 MHz, DMSO-d_6): δ12.77 (s, 1H, -NH), 10.69 (s, 1H, -NH), 9.77 (s, 1H, -OH), 7.92 (s, 1H, oxazole-H), 7.68–7.63 (m, 2H, H-4/H-7), 7.58 (d, $J_{(2', 3'/ 6', 5')}$ = 9.1 Hz, 2H, H-2′/H-6′), 7.48 (d, $J_{(2'', 3''/ 6'', 5'')}$ = 7.0 Hz, 2H, H-2″/H-6″), 7.36–7.29 (m, 2H, H-5/H-6), 7.17 (d, $J_{(3', 2'/5', 6')}$ = 8.3 Hz, 2H, H-3′/H-5′), 6.96 (d, $J_{(3'', 2''/5'', 6'')}$ = 8.2 Hz, 2H, H-3″/H-5″), 4.01 (s, 2H, S-CH_2), 2.31 (s, 3H, -CH_3).; ^{13}C-NMR (150 MHz, DMSO-d6): δ 159.5, 155.0, 150.0, 146.5, 142.5, 139.5, 139.3, 138.3, 138.1, 132.8, 130.9, 130.9, 129.9, 129.9, 128.8, 128.8, 124.3, 122.4, 122.1, 117.4, 117.4, 114.6, 114.4, 36.9, 23.1.; HR-MS (ESI): (*m*/*z*) [M + H]$^+$ calculated for $C_{25}H_{22}N_5O_2S$ 456.1488, found 456.1499.

3.2.10. (*E*)-2-(2-(2-((1H-Benzo[d]imidazol-2-yl)thio)-1-phenylethylidene)hydrazinyl)-4-(3-nitrophenyl)oxazole (**10**)

Yield: 73%; Rf value 0.57 (7:3 n-hex: EtOAc); ^{1} H NMR (600 MHz, DMSO-d_6): δ12.82 (s, 1H, -NH), 10.74 (s, 1H, -NH), 8.52 (t, $J_{(2''/4'', 6'')}$ = 2.5 Hz, 1H, H-2″), 8.34 (d, $J_{(6'', 5'')}$ = 9.0 Hz, 1H, H-6″), 8.21–8.17 (m, 1H, H-4″), 8.07–8.01 (m, 2H, H-2′/H-6′), 7.88 (t, $J_{(5''/4'', 6'')}$ = 8.1 Hz, 1H, H-5″), 7.78 (s, 1H, oxazole-H), 7.72 (m, 2H, H-4/H-7), 7.57–7.51 (m, 3H, H-3′/H-4′/H-5′), 7.41 (m, 2H, H-5/H-6), 4.06 (s, 2H, S-CH_2).; ^{13}C-NMR (150 MHz, DMSO-d6): δ 157.0, 152.0, 148.8, 148.5, 141.5, 141.3, 140.3, 140.1, 136.0, 134.3, 134.0, 133.0, 131.0, 130.8, 130.8, 130.2, 130.2, 124.5, 124.3, 124.0, 123.1, 116.6, 116.4, 38.9.; HR-MS (ESI): (*m*/*z*) [M + H]$^+$ calculated for $C_{24}H_{19}N_6O_3S$ 471.1237, found 471.1245.

3.2.11. (*E*)-2-(2-(2-((1H-Benzo[d]imidazol-2-yl)thio)-1-(4-chlorophenyl)ethylidene)hydrazi-nyl)-4-(3-nitrophenyl)oxazole (**11**)

Yield: 79%; Rf value 0.61 (7:3 n-hex: EtOAc); ^{1} H NMR (600 MHz, DMSO-d_6): δ12.68 (s, 1H, -NH), 10.60 (s, 1H, -NH), 8.50 (t, $J_{(2''/4'', 6'')}$ = 2.0 Hz, 1H, H-2″), 8.31 (d, $J_{(6'', 5'')}$ = 7.7 Hz, 1H, H-6″), 8.19–8.13 (m, 1H, H-4″), 8.08 (d, $J_{(2', 3'/ 6', 5')}$ = 9.0 Hz, 2H, H-2′/H-6′), 7.86 (t, $J_{(5''/4'', 6'')}$ = 7.5Hz, 1H, H-5″), 7.83 (s, 1H, oxazole-H), 7.72 (d, $J_{(3', 2'/5', 6')}$ = 8.4 Hz, 2H, H-3′/H-5′), 7.58 (m, 2H, H-4/H-7), 7.27 (m, 2H, H-5/H-6), 3.91 (s, 2H, S-CH_2).; ^{13}C-NMR (150 MHz, DMSO-d6): δ. 166.1, 163.1, 149.8, 41.2, 133.1, 132.2, 131.6, 131.6, 131.5, 130.5, 127.8, 127.6,127.5, 122.4, 122.3, 121.3, 120.9, 119.8, 119.6,111.0, 107.5, 40.0; HR-MS (ESI): (*m*/*z*) [M + H]$^+$ calculated for $C_{24}H_{18}ClN_6O_3S$ 508.0846, found 508.0855.

3.2.12. (*E*)-2-(2-(2-((1H-Benzo[d]imidazol-2-yl)thio)-1-(*p*-tolyl)ethylidene)hydrazinyl)-4-(4-chlorophenyl)oxazole (**12**)

Yield: 72%; Rf value 0.65 (7:3 n-hex: EtOAc); ^{1} H NMR (600 MHz, DMSO-d_6): δ12.70 (s, 1H, -NH), 10.62 (s, 1H, -NH), 8.08 (d, $J_{(2'', 3''/ 6'', 5'')}$ = 6.9 Hz, 2H, H-2″/H-6″), 7.85 (s, 1H, oxazole-H), 7.75 (d, $J_{(2', 3'/ 6', 5')}$ = 8.8 Hz, 2H, H-2′/H-6′), 7.63 (d, $J_{(3'', 2''/5'', 6'')}$ = 7.7 Hz, 2H, H-3″/H-5″), 7.57–7.50 (m, 2H, H-4/H-7), 7.34 (d, $J_{(3', 2'/5', 6')}$ = 9.4 Hz, 2H, H-3′/H-5′), 7.28–7.18 (m, 2H, H-5/H-6), 3.93 (s, 2H, S-CH_2), 2.47 (s, 3H, -CH_3).; ^{13}C-NMR (150 MHz, DMSO-d6): δ 166.1, 163.0, 161.3, 159.4, 156.7, 153.5, 136.9, 136.8, 135.7, 130.9, 130.9, 130.8, 129.4, 129.3, 128.8, 128.3, 127.9, 127.7, 126.2, 124.2, 122.2, 120.6, 117.5, 117.4, 115.7, 113.8, 113.7, 64.8, 15.1; HR-MS (ESI): (*m*/*z*) [M + H]$^+$ calculated for $C_{25}H_{21}N_6O_3S$ 485.1393, found 485.1401.

3.2.13. (*E*)-2-(2-(2-((1H-Benzo[d]imidazol-2-yl)thio)-1-(*p*-tolyl)ethylidene)hydrazinyl)-4-phenyloxazole (**13**)

Yield: 68%; Rf value 0.54 (7:3 n-hex: EtOAc); ^{1} H NMR (600 MHz, DMSO-d_6): δ12.79 (s, 1H, -NH), 10.71 (s, 1H, -NH), 7.97 (s, 1H, oxazole-H), 7.91–7.85 (m, 2H, H-2″/H-6″), 7.80 (d, $J_{(2', 3'/ 6', 5')}$ = 7.1 Hz, 2H, H-2′/H-6′), 7.74–7.68 (m, 2H, H-4/H-7), 7.63–7.56 (m, 3H, H-3″/H-4″/H-5″), 7.46 (d, $J_{(3', 2'/5', 6')}$ = 6.9 Hz, 2H, H-3′/H-5′), 7.38–7.31 (m, 2H, H-5/H-6), 4.03 (s, 2H, S-CH_2), 2.54 (s, 3H, -CH_3).; ^{13}C-NMR (150 MHz, DMSO-d6): δ 155.5, 150.5, 147.0,

143.4, 140.0, 139.8, 138.8, 138.6, 132.7, 131.7, 130.8, 130.8, 130.2, 130.2, 129.7, 128.7, 128.7, 125.7, 125.7, 122.9, 122.6, 115.1, 114.9, 37.4, 22.8.; HR-MS (ESI): (*m*/*z*) $[M + H]^+$ calculated for $C_{25}H_{21}ClN_5OS$ 474.1151, found 474.1161.

3.2.14. (*E*)-2-(2-(2-((1H-Benzo[d]imidazol-2-yl)thio)-1-(*p*-tolyl)ethylidene)hydrazinyl)-4-(2,4-dichlorophenyl)oxazole (**14**)

Yield: 80%; Rf value 0.57 (7:3 n-hex: EtOAc); ^{1} H NMR (600 MHz, DMSO-d_6): δ12.77 (s, 1H, -NH), 10.69 (s, 1H, -NH), 8.13 (d, $J_{(6'', 5'')}$ =8.8 Hz, 1H, H-6″), 7.92 (s, 1H, oxazole-H), 7.79 (d, $J_{(2', 3'/ 6', 5')}$ = 7.8 Hz, 2H, H-2′/H-6′), 7.67–7.63 (m, 2H, H-4/H-7), 7.59 (d, $J_{(3'', 5'')}$ = 1.6 Hz, 1H, H-3″), 7.46 (dd, $J_{(5'', 6'')}$ = 8.4 Hz, $J_{(5'', 3'')}$ =1.8 Hz, 1H, H-5″), 7.41 (d, $J_{(3', 2'/5', 6')}$ = 7.9 Hz, 2H, H-3′/H-5′), 7.36–7.30 (m, 2H, H-5/H-6), 4.01 (s, 2H, S-CH_2), 2.51 (s, 3H, -CH_3).; ^{13}C-NMR (150 MHz, DMSO-d6): δ 157.5, 152.5, 149.0, 143.3, 142.0, 141.8, 140.8, 140.6, 136.7, 134.6, 132.6, 131.9, 131.3, 130.7, 130.7, 129.0, 128.6, 128.6, 128.4, 124.9, 124.6, 117.1, 116.9, 39.4, 22.9.; HR-MS (ESI): (*m*/*z*) $[M + H]^+$ calculated for $C_{25}H_{20}Cl_2N_5OS$ 508.0763, found 508.0771.

3.2.15. (*E*)-2-(2-(2-((1H-Benzo[d]imidazol-2-yl)thio)-1-phenylethylidene)hydrazinyl)-4-(3-methoxyphenyl)oxazole (**15**)

Yield: 74%; Rf value 0.60 (7:3 n-hex: EtOAc); ^{1} H NMR (600 MHz, DMSO-d_6): δ12.71 (s, 1H, -NH), 10.63 (s, 1H, -NH), 7.86–7.79 (m, 2H, H-2′/H-6′), 7.73 (s, 1H, oxazole-H), 7.69–7.64 (m, 1H, H-6″), 7.60 (m, 2H, H-4/H-7), 7.51 (dd, $J_{(5'', 4'')}$ = 9.0 Hz, $J_{(5'', 6'')}$ = 9.3 Hz, 1H, H-5″), 7.47–7.38 (m, 3H, H-3′/H-4′/H-5′), 7.36 (t, $J_{(2''/4'', 6'')}$ = 2.6Hz, 1H, H-2″), 7.30 (m, 2H, H-5/H-6), 7.13 (d, $J_{(4'', 5'')}$ = 8.4 Hz, 1H, H-4″), 3.95 (s, 2H, S-CH_2), 3.89 (s, 3H, -OCH_3).; ^{13}C-NMR (150 MHz, DMSO-d6): δ 161.6, 155.1, 150.1, 146.6, 139.6, 139.4, 138.4, 138.2, 136.5, 134.5, 133.5, 131.3, 131.3, 130.9, 130.7, 130.7, 122.5, 122.2, 120.3, 114.9, 114.7, 114.5, 114.1, 56.3, 37.0.; HR-MS (ESI): (*m*/*z*) $[M + H]^+$ calculated for $C_{25}H_{22}N_5O_2S$ 456.1487, found 456.1499.

3.2.16. (*E*)-2-(2-(2-((1H-Benzo[d]imidazol-2-yl)thio)-1-([1,1′-biphenyl]-4-yl)ethylidene) Hydrazinyl)-4-(*p*-tolyl)oxazole (**16**)

Yield: 67%; Rf value 0.52 (7:3 n-hex: EtOAc); ^{1} H NMR (600 MHz, DMSO-d_6): δ11.27 (s, 1H, -NH), 10.04 (s, 1H, -NH), 8.27 (d, $J_{(2', 3'/ 6', 5')}$ = 7.9 Hz, 2H, H-2′/H-6′), 8.15 (d, $J_{(3', 2'/5', 6')}$ = 8.5 Hz, 2H, H-3′/H-5′), 7.99 (s, 1H, oxazole-H), 7.63 (d, $J_{(2'', 3''/ 6'', 5'')}$ = 8.7 Hz, 2H, H-2″/H-6″), 7.54 (d, $J_{(3'', 2''/5'', 6'')}$ = 8.1 Hz, 2H, H-3″/H-5″), 7.35–7.03 (m, 2H, H-4/H-7), 6.97–6.89 (m, 5H, *para*-Ph), 6.77–6.75 (m, 2H, H-5/H-6), 2.50 (s, 2H, S-CH_2), 1.23 (s, 3H, -CH_3).; ^{13}C-NMR (150 MHz, DMSO-d6): δ 156.8, 151.8, 148.3, 143.6, 141.6, 141.3, 141.1, 140.1, 139.9, 133.3, 132.1, 129.9, 129.9, 129.7, 129.7, 129.5, 129.5, 128.5, 128.5, 128.1, 127.8, 127.7, 127.7, 126.1, 126.1, 124.2, 123.9, 116.4, 116.2, 38.7, 21.7.; HR-MS (ESI): (*m*/*z*) $[M + H]^+$ calculated for $C_{31}H_{26}N_5OS$ 485.1854, found 516.1863.

3.2.17. (*E*)-2-(2-(2-((1H-Benzo[d]imidazol-2-yl)thio)-1-phenylethylidene)hydrazinyl)-4-(2-nitrophenyl)oxazole (**17**)

Yield: 81%; Rf value 0.62 (7:3 n-hex: EtOAc); ^{1} H NMR (600 MHz, DMSO-d_6): δ12.67 (s, 1H, -NH), 10.59 (s, 1H, -NH), 8.57 (t, $J_{(2''/4'', 6'')}$ = 2.8Hz, 1H, H-2″), 8.38 (d, $J_{(6'', 5'')}$ = 6.6Hz, 1H, H-6″), 8.27–8.19 (m, 1H, H-4″), 7.99–7.94 (m, 2H, H-2′/H-6′), 7.91 (t, $J_{(5''/4'',6'')}$ = 7.8Hz, 1H, H-5″), 7.82 (s, 1H, oxazole-H), 7.57–7.51 (m, 2H, H-4/H-7), 7.48–7.39 (m, 3H, H-3′/H-4′/H-5′), 7.26–7.18 (m, 2H, H-5/H-6), 3.90 (s, 2H, S-CH_2).; ^{13}C-NMR (150 MHz, DMSO-d6): δ 157.7, 152.7, 149.4, 149.2, 142.2, 142.0, 141.0, 140.8, 136.3, 136.1, 133.2, 133.0, 131.0, 131.0, 130.7, 130.5, 130.3, 125.6, 125.4, 125.1, 124.8, 117.3, 117.1, 39.6.; HR-MS (ESI): (*m*/*z*) $[M + H]^+$ calculated for $C_{24}H_{19}N_6O_3S$ 471.1237, found 471.1245.

3.2.18. (*E*)-2-(2-(2-((1H-Benzo[d]imidazol-2-yl)thio)-1-(4-chlorophenyl)ethylidene)hydrazinyl)-4-(2-nitrophenyl)oxazole (**18**)

Yield: 83%; Rf value 0.58 (7:3 n-hex: EtOAc); ^{1} H NMR (600 MHz, DMSO-d_6): δ12.74 (s, 1H, -NH), 10.66 (s, 1H, -NH), 8.52 (t, $J_{(2''/4'', 6'')}$ = 1.8Hz, 1H, H-2″), 8.31 (d, $J_{(6'', 5'')}$ = 6.9 Hz, 1H, H-6″), 8.24–8.17 (m, 1H, H-4″), 8.09 (d, $J_{(2', 3'/ 6', 5')}$ = 9.5 Hz, 2H, H-2′/H-6′),7.90 (t, $J_{(5''/4'', 6'')}$ = 8.6 Hz, 1H, H-5″), 7.87 (s, 1H, oxazole-H), 7.77 (d, $J_{(3', 2'/5', 6')}$ = 8.6 Hz, 2H, H-3′/H-5′), 7.64–7.56 (m, 2H, H-4/H-7), 7.33–7.25 (m, 2H, H-5/H-6), 3.97 (s, 2H, S-CH_2).; ^{13}C-NMR (150 MHz, DMSO-d6): δ 157.8, 152.8, 149.3, 149.1, 142.3, 141.1, 141.1, 140.9, 138.4, 136.1, 133.5, 133.0, 130.8, 130.8, 130.6, 130.1, 130.1, 125.8, 125.4, 125.2, 124.9, 117.4, 117.2, 39.7.; HR-MS (ESI): (*m*/*z*) [M + H]$^+$ calculated for $C_{24}H_{18}ClN_6O_3S$ 508.0846, found 508.0855.

3.2.19. (*E*)-2-(2-(2-((1H-Benzo[d]imidazol-2-yl)thio)-1-(4-chlorophenyl)ethylidene)hydrazinyl)-4-(3-methoxyphenyl)oxazole (**19**)

Yield: 79%; Rf value 0.56 (7:3 n-hex: EtOAc); ^{1} H NMR (600 MHz, DMSO-d_6): δ12.78 (s, 1H, -NH), 10.70 (s, 1H, -NH), 8.07 (d, $J_{(2', 3'/ 6', 5')}$ = 9.2 Hz, 2H, H-2′/H-6′), 7.93 (s, 1H, oxazole-H), 7.74 (d, $J_{(3', 2'/5', 6')}$ = 7.9 Hz, 2H, H-3′/H-5′), 7.68 (m, 2H, H-4/H-7), 7.63–7.56 (m, 1H, H-6″), 7.50 (dd, $J_{(5'', 4'')}$ = 8.3 Hz, $J_{(5'', 6'')}$ = 8.9 Hz, 1H, H-5″), 7.39 (t, $J_{(2''/4'', 6'')}$ = 1.8Hz, 1H, H-2″), 7.34–7.28 (m, 2H, H-5/H-6), 7.12 (d, $J_{(4'', 5'')}$ = 7.5 Hz, 1H, H-4″), 4.02 (s, 2H, S-CH_2), 3.89 (s, 3H, -OCH_3).; ^{13}C-NMR (150 MHz, DMSO-d6): δ 161.9, 157.3, 152.3, 148.8, 141.8, 141.6, 140.6, 140.4, 138.7, 134.7, 133.2, 131.0, 131.0, 130.9, 130.3, 130.3, 124.7, 124.4, 120.6, 116.9, 116.7, 115.0, 114.4, 56.7, 39.2.; HR-MS (ESI): (*m*/*z*) [M + H]$^+$ calculated for $C_{25}H_{21}ClN_5O_2S$ 490.1098, found 490.1109.

3.3. Assay Protocol for Acetylcholinesterase and Butyrylcholinesterase Activities

According to previously established protocols, in vitro AChE and BuChE inhibition profiles were evaluated with slight modifications [33,34].

3.4. Protocol for Molecular Docking Study

In order to properly triangulate the in vitro and in silico results, a molecular docking analysis was carried out using the AutoDock Vina software (version 1.5.7) package to understand the binding mode of synthetic compounds against both the targeted AChE and BuChE enzymes. The RCSB protein databank's crystal structures for both targets were obtained using the PDB codes 1ACL for AChE and 1P0P for BuChE. The crystallographic structures and all of the produced compounds were protonated and energy was reduced using the default MOE-Dock module parameters, resulting in optimized enzyme and compound structures. Docking research was then conducted using the improved enzyme and chemical structures. Our prior investigations covered all of the docking protocol's specifics in depth [35,36].

4. Conclusions

In conclusion, we synthesized benzimidazole-based oxazole derivatives (1–19) and evaluated them against both AChE and BuChE enzymes, respectively. All of the synthesized analogues were evaluated for their inhibition profiles against the AChE and BuChE enzymes as compared to donepezil, the standard drug. All of the synthesized benzimidazole-based oxazole analogues showed a varied range of inhibitory potentials against targeted AChE and BuChE enzymes, with IC_{50} values ranging from 0.10 ± 0.050 to 12.60 ± 0.30 μM (for AChE) and 0.20 ± 0.050 μM to 16.30 ± 0.30 μM (for BuChE) when compared to standard donepezil (IC_{50} = 2.16 ± 0.12 μM for AChE) and 4.50 ± 0.11 μM for BuChE). Structure-activity relationship (SAR) studies revealed that analogues 9 (bearing *para*-CF_3 on ring B and *meta*-NO_2 substitution at ring C) and 14 (that holds *para*-CH_3 substitutions on ring B and 2,4-diCl moieties on ring C) were the most potent analogues of the AChE and BuChE enzymes, with IC_{50} values of 0.10 ± 0.050 and 0.20 ± 0.050 μM (against AChE) and 0.20 ± 0.050 and 0.30 ± 0.050 μM (against BuChE), respectively. In

order to explore the binding interactions possessed by active scaffolds with the active sites of amino acids of the targeted AChE and BuChE enzymes, the active analogues were also subjected to molecular docking studies. The results revealed that these active analogues provided numerous important interactions with the targeted enzymes' active sites. All of the synthesized analogues were structurally elucidated using spectroscopic methods such as ^{1}H-NMR, ^{13}C-NMR, and HREI-MS.

Supplementary Materials: The following supporting information can be downloaded at: https://www.mdpi.com/article/10.3390/molecules28207015/s1. Figure S1: 1HNMR for the compound **2**; Figure S2: 13CNMR for the compound **4**; Figure S3: 1HNMR for the compound **7**; Figure S4: 13CNMR for the compound **11**; Figure S5: 13CNMR for the compound **12**; Figure S6: 1HNMR for the compound **16**.

Author Contributions: Conceptualization, F.R. and H.U.; methodology, R.H.; software, S.K.; validation, M.S. and R.I.; formal analysis, H.U.; investigation, H.U. and F.R.; data curation, M.S. and F.S.; writing—original draft preparation, R.H. and H.U.; writing—review and editing, R.I., F.S., M.S. and M.K.A.-S.; project administration, F.R. and H.U. All authors have read and agreed to the published version of the manuscript.

Funding: Supported by the Researchers Supporting Project Number (RSP2023R410), King Saud University, Riyadh, Saudi Arabia.

Acknowledgments: The authors would like to extend their sincere appreciation to the Researchers Supporting Project Number (RSP2023R410), King Saud University, Riyadh, Saudi Arabia.

Conflicts of Interest: The authors declare no conflict of interest.

References

1. Millard, C.B.; Broomfield, C.A. Anticholinesterases: Medical application of neurochemical principles. *J. Neurochem.* **1995**, *64*, 1909–1918. [CrossRef]
2. Milatovifil, D.; Dettbarn, W.D. The role of carboxylesterase in toxicity and tolerance to organophosphorus anticholinesterases paraoxon and DFP. *Toxicol. Appl. Pharmacol.* **1966**, *136*, 20–28.
3. Weinstock, M.; Groner, E. Rational design of a drug for Alzheimer's disease with cholinesterase inhibitory and neuroprotective activity. *Chem.-Biol. Interact.* **2008**, *175*, 216–221. [CrossRef]
4. Jann, M.W. Preclinical pharmacology of metrifonate. *Pharmacother. J. Hum. Pharmacol. Drug Ther.* **1998**, *18*, 55–67.
5. Massoulié, J.; Pezzementi, L.; Bon, S.; Krejci, E.; Vallette, F.M. Molecular and cellular biology of cholinesterases. *Prog. Neurobiol.* **1993**, *41*, 31–91. [CrossRef] [PubMed]
6. Aisen, P.S.; Davis, K.L. The search for disease-modifying treatment for Alzheimer's disease. *Neurology* **1997**, *48* (Suppl. 6), 35S–41S. [CrossRef]
7. Whitehouse, P.J.; Price, D.L.; Struble, R.G.; Clark, A.W.; Coyle, J.T.; DeLong, M.R. Alzheimer's disease and senile dementia: Loss of neurons in the basal forebrain. *Science* **1982**, *215*, 1237–1239. [CrossRef]
8. Ullah, H.; Bibi, U.; Hussain, A.; Sarfraz, M.; Rahim, F.; Hayat, S.; Zada, H.; Khan, F.; Wadood, A. Synthesis and Molecular Docking Study of Bis-Indolylmethane Thiourea Derivatives as Anti-Alzheimer Agents. *Russ. J. Org. Chem.* **2023**, *59*, 181–189. [CrossRef]
9. Maruish, M.E.; Moses, J.A. *Clinical Neuropsychology: Theoretical Foundations for Practitioners*; Psychology Press: London, UK, 2013; p. 371.
10. Schetinger, M.R.; Porto, N.M.; Moretto, M.B.; Morsch, V.M.; da Rocha, J.B.T.; Vieira, V.; Moro, F.; Neis, R.T.; Bittencourt, S.; Bonacorso, H.G.; et al. New benzodiazepines alter acetylcholinesterase and ATPDase activities. *Neurochem. Res.* **2000**, *25*, 949–955. [CrossRef]
11. Prandota, J. Unexplained liver damage, cryptogenic liver cirrhosis, and steatohepatitis may be caused by latent chronic toxoplasmosis. *Toxicol. Appl. Pharmacol.* **1973**, *24*, 29–100. [CrossRef]
12. Kubo, K.; Inada, Y.; Kohara, Y.; Sugiura, Y.; Ojima, M.; Itoh, K.; Furukawa, Y.; Nishikawa, K.; Naka, T. Nonpeptide angiotensin II receptor antagonists. Synthesis and biological activity of benzimidazoles. *J. Med. Chem.* **1993**, *36*, 1772–1784. [CrossRef]
13. Sabat, M.; VanRens, J.C.; Laufersweiler, M.J.; Brugel, T.A.; Maier, J.; Golebiowski, A.; De, B.; Easwaran, V.; Hsieh, L.C.; Walter, R.L.; et al. The development of 2-benzimidazole substituted pyrimidine based inhibitors of lymphocyte specific kinase (Lck). *Bioorganic Med. Chem. Lett.* **2006**, *16*, 5973–5977. [CrossRef] [PubMed]
14. Güven, Ö.Ö.; Erdoğan, T.; Göker, H.; Yıldız, S. Synthesis and antimicrobial activity of some novel phenyl and benzimidazole substituted benzyl ethers. *Bioorganic Med. Chem. Lett.* **2007**, *17*, 2233–2236. [CrossRef]
15. Townsend, L.B.; Devivar, R.V.; Turk, S.R.; Nassiri, M.R.; Drach, J.C. Design, synthesis, and antiviral activity of certain 2,5,6-Trihalo-1-(.beta.-D-ribofuranosyl) benzimidazoles. *J. Med. Chem.* **1995**, *38*, 4098–4105. [CrossRef]

16. Valdez, J.; Cedillo, R.; Hernández-Campos, A.; Yepez, L.; Hernández-Luis, F.; Navarrete-Vazquez, G.; Tapia, A.; Cortés, R.; Hernández, M.; Castillo, R. Synthesis and antiparasitic activity of 1*H*-benzimidazole derivatives. *Bioorganic Med. Chem. Lett.* **2002**, *12*, 2221–2224. [CrossRef]
17. Kuş, C.; Ayhan-Kılcıgil, G.; Özbey, S.; Kaynak, F.B.; Kaya, M.; Çoban, T.; Can-Eke, B. Synthesis and antioxidant properties of novel *N*-methyl-1,3,4-thiadiazol-2-amine and 4-methyl-2*H*-1,2,4-triazole-3 (4*H*)-thione derivatives of benzimidazole class. *Bioorganic Med. Chem.* **2008**, *16*, 4294–4303. [CrossRef]
18. Arnaiz, D.O.; Liang, A.; Trinh, L.; Whitlow, M.; Koovakkat, S.K.; Shaw, K.J. Design, synthesis, and in vitro biological activity of indole-based factor Xa inhibitors. *Bioorganic Med. Chem. Lett.* **2000**, *10*, 957–961. [CrossRef]
19. Selvakumar, S.; Babu, I.S.; Chidambaranathan, N. In-Vivo Central Nervous System-Locomotor Activity of Some Synthesized 2-[(1-((phenyl amino) methyl) Substituted 1-benzoimidazol-2-yl) alkyl] Isoindoline-1,3-diones. *Biosci. Biotech. Res. Asia* **2013**, *10*, 937–943. [CrossRef]
20. Schulz, W.G.; Islam, I.; Skibo, E.B. Pyrrolo [1,2-a] benzimidazole-based quinones and iminoquinones. The role of the 3-substituent on cytotoxicity. *J. Med. Chem.* **1995**, *38*, 109–118. [CrossRef]
21. Bansal, Y.; Silakari, O. The therapeutic journey of benzimidazoles: A review. *Bioorganic Med. Chem.* **2012**, *20*, 6208–6236. [CrossRef]
22. Zhou, R.R.; Cai, Q.; Li, D.K.; Zhuang, S.Y.; Wu, Y.D.; Wu, A.X. Acid-Promoted Multicomponent Tandem Cyclization to Synthesize Fully Substituted Oxazoles via Robinson–Gabriel-Type Reaction. *J. Org. Chem.* **2017**, *82*, 6450–6456. [CrossRef]
23. Taha, M.; Sadia, H.; Rahim, F.; Khan, M.I.; Hayat, S.; Iqbal, N.; Nawaz, F.; Ullah, H.; Zada, H.; Shah, S.A.A.; et al. Synthesis, biological evaluation and molecular docking study of oxindole based chalcone analogues as potent anti-Alzheimer agents. *J. Mol. Struct.* **2023**, *1285*, 135530. [CrossRef]
24. Kakkar, S.; Kumar, S.; Lim, S.M.; Ramasamy, K.; Mani, V.; Shah, S.A.A.; Narasimhan, B. Design, synthesis and biological evaluation of 3-(2-aminooxazol-5-yl)-2*H*-chromen-2-one derivatives. *Chem. Cent. J.* **2018**, *12*, 130. [CrossRef]
25. Khan, S.; Iqbal, S.; Khan, M.; Rehman, W.; Shah, M.; Hussain, R.; Rasheed, L.; Khan, Y.; Dera, A.A.; Pashameah, R.A.; et al. Design, synthesis, in silico testing, and in vitro evaluation of thiazolidinone-based benzothiazole derivatives as inhibitors of α-amylase and α-glucosidase. *Pharmaceuticals* **2022**, *15*, 1164. [CrossRef]
26. Mumtaz, S.; Iqbal, S.; Shah, M.; Hussain, R.; Rahim, F.; Rehman, W.; Khan, S.; Abid, O.U.R.; Rasheed, L.; Dera, A.A.; et al. New triazinoindole bearing benzimidazole/benzoxazole hybrids analogs as potent inhibitors of urease: Synthesis, in vitro analysis and molecular docking studies. *Molecules* **2022**, *27*, 6580. [CrossRef]
27. Rahim, F.; Ullah, H.; Taha, M.; Hussain, R.; Sarfraz, M.; Iqbal, R.; Iqbal, N.; Khan, S.; Ali Shah, S.A.; Albalawi, M.A.; et al. Synthesis of new triazole-based thiosemicarbazone derivatives as anti-Alzheimer's disease candidates: Evidence-based in vitro study. *Molecules* **2022**, *28*, 21. [CrossRef]
28. Alpan, A.S.; Parlar, S.; Carlino, L.; Tarikogullari, A.H.; Alptüzün, V.; Güneş, H.S. Synthesis, biological activity and molecular modeling studies on 1*H*-benzimidazole derivatives as acetylcholinesterase inhibitors. *Bioorganic Med. Chem.* **2013**, *21*, 4928–4937. [CrossRef]
29. Hussain, R.; Ullah, H.; Rahim, F.; Sarfraz, M.; Taha, M.; Iqbal, R.; Rehman, W.; Khan, S.; Shah, S.A.A.; Hyder, S.; et al. Multipotent cholinesterase inhibitors for the treatment of Alzheimer's disease: Synthesis, biological analysis and molecular docking study of benzimidazole-based thiazole derivatives. *Molecules* **2022**, *27*, 6087. [CrossRef] [PubMed]
30. Coban, G.; Carlino, L.; Tarikogullari, A.H.; Parlar, S.; Sarıkaya, G.; Alptüzün, V.; Alpan, A.S.; Güneş, H.S.; Erciyas, E. 1*H*-benzimidazole derivatives as butyrylcholinesterase inhibitors: Synthesis and molecular modeling studies. *Med. Chem. Res.* **2016**, *25*, 2005–2014. [CrossRef]
31. Šagud, I.; Maček Hrvat, N.; Grgičević, A.; Čadež, T.; Hodak, J.; Dragojević, M.; Lasić, K.; Kovarik, Z.; Škorić, I. Design, synthesis and cholinesterase inhibitory properties of new oxazole benzylamine derivatives. *J. Enzym. Inhib. Med. Chem.* **2020**, *35*, 460–467. [CrossRef] [PubMed]
32. Hussain, R.; Khan, S.; Ullah, H.; Ali, F.; Khan, Y.; Sardar, A.; Iqbal, R.; Ataya, F.S.; El-Sabbagh, N.M.; Batiha, G.E.S. Benzimidazole-Based Schiff Base Hybrid Scaffolds: A Promising Approach to Develop Multi-Target Drugs for Alzheimer's Disease. *Pharmaceuticals* **2023**, *16*, 1278. [CrossRef] [PubMed]
33. Chigurupati, S.; Selvaraj, M.; Mani, V.; Selvarajan, K.K.; Mohammad, J.I.; Kaveti, B.; Bera, H.; Palanimuthu, V.R.; Teh, L.K.; Salleh, M.Z. Identification of novel acetylcholinesterase inhibitors: Indolopyrazoline derivatives and molecular docking studies. *Bioorganic Chem.* **2016**, *67*, 9–17. [CrossRef]
34. Chigurupati, S.; Selvaraj, M.; Mani, V.; Mohammad, J.I.; Selvarajan, K.K.; Akhtar, S.S.; Marikannan, M.; Raj, S.; Teh, L.K.; Salleh, M.Z. Synthesis of azomethines derived from cinnamaldehyde and vanillin: In vitro aetylcholinesterase inhibitory, antioxidant and insilico molecular docking studies. *Med. Chem. Res.* **2018**, *27*, 807–816. [CrossRef]
35. Wadood, A.; Shareef, A.; Ur Rehman, A.; Muhammad, S.; Khurshid, B.; Khan, R.S.; Shams, S.; Afridi, S.G. In silico drug designing for ala438 deleted ribosomal protein S1 (RpsA) on the basis of the active compound Zrl15. *ACS Omega* **2021**, *7*, 397–408. [CrossRef]
36. Rehman, A.U.; Zhen, G.; Zhong, B.; Ni, D.; Li, J.; Nasir, A.; Gabr, M.T.; Rafiq, H.; Wadood, A.; Lu, S.; et al. Mechanism of zinc ejection by disulfiram in nonstructural protein 5A. *Phys. Chem. Chem. Phys.* **2021**, *23*, 12204–12215. [CrossRef] [PubMed]

Disclaimer/Publisher's Note: The statements, opinions and data contained in all publications are solely those of the individual author(s) and contributor(s) and not of MDPI and/or the editor(s). MDPI and/or the editor(s) disclaim responsibility for any injury to people or property resulting from any ideas, methods, instructions or products referred to in the content.